UNIVERSITY OF CALIFORNIA SAN DIEGO

A CRISPRi screen to identify pathways of Leucine Rich Repeat Kinase 2 protein degradation in vivo

A Thesis submitted in partial satisfaction of the requirements
for the degree Master of Science

in

Biology

by

Yiyi Shen

Committee in charge:

Professor Annie Hiniker, Chair
Professor Samara Reck-Peterson, Co-Chair
Professor Eric Bennett,

The Thesis of Yiyi Shen is approved, and it is acceptable in quality and form for publication on microfilm and electronically.

University of California San Diego

2022

TABLE OF CONTENTS

LIST OF FIGURES

ACKNOWLEDGEMENTS

I would like to thank Dr. Annie Hiniker for her support and mentorship for the last three years.

I would also like to acknowledge my collaborator Biswarathan Ramani for helping me conduct the CRISPRi screen.

I would also like to thank the members of the Hiniker lab, especially Alexandra Unapanta and Farbod Shavarebi for giving me valuable feedback on the thesis.

Chapter 3 of this thesis contains unpublished data co-authored with Biswarathan Ramani at the Martin Kampmann lab from UCSF. The thesis author was the primary researcher of this chapter.

ABSTRACT OF THE THESIS

A CRISPRi screen to identify pathways of Leucine Rich Repeat Kinase 2 protein degradation in vivo

By

Yiyi Shen

Master of Science in Biology

University of California San Diego, 2022

Professor Annie Hiniker, Chair

Professor Samara Reck-Peterson, Co-Chair

Parkinson's disease (PD) is a neurodegenerative movement disorder that affects roughly 1% of the population over 60. Point mutations in the LRRK2 gene are the most common cause of late-onset familial PD. Various studies have implicated LRRK2 kinase activity and LRRK2 protein level as key drivers of LRRK2 toxicity. Moreover, LRRK2 kinase inhibition can drive LRRK2 proteasomal degradation; however, the pathways by which this process occurs are

unidentified. Therefore, delineating the mechanism controlling LRRK2 protein degradation should give valuable insights into understanding PD pathogenesis as well as possible new therapeutic approaches. The main goal of this thesis is to identify novel proteins that mediate LRRK2 turnover. Chapter 1 introduces LRRK2 and provides background into what is known about its cellular function and degradation. For Chapter 2, I tested the hypothesis that PJA2 and BIRC2, two proteins previously identified to regulate LRRK2 levels, catalyze LRRK2 turnover after kinase inhibition; however, I was unable to validate the result, which suggested that LRRK2 turnover after kinase inhibition occurs through another unidentified mechanism. Therefore, for chapter 3, we conducted a CRISPRi screen utilizing protein-coding genes relevant to the ubiquitin-proteasome system to identify pathways regulating LRRK2 protein levels in the presence and absence of kinase inhibition. From the screen, we identified two ubiquitination-like pathways, SUMOylation and neddylation, as potential pathways that regulate LRRK2 levels. I have validated single-gene members of these pathways as regulators of LRRK2 protein levels in an overexpression system. Next steps will test the effects of these regulators on endogenous LRRK2 levels. In summary, this thesis identifies novel potential regulatory pathways that drive LRRK2 protein degradation in the presence and absence of LRRK2 kinase inhibition.

CHAPTER 1 Overview of LRRK2 Biology

Parkinson's disease (PD) is a neurodegenerative movement disorder that affects around 7 million people worldwide. PD results from degeneration of dopaminergic neurons in the substantia nigra, leading to motor deficits including resting tremor, bradykinesia and postural instability (1). PD patients can also develop symptoms unrelated to movement such as depression, sleep disruption, and dementia (2). On a cellular level, PD is often associated with protein aggregates called Lewy bodies. The primary molecular component of Lewy bodies is α-synuclein but also includes other insoluble proteins such as ubiquitin (3). Reports have demonstrated that oligomers of α-synuclein can be cytotoxic, therefore protein aggregation may be a protective mechanism in PD (4). The formation of Lewy bodies is hypothesized to be related to aggresomes, which is a cytoprotective proteinaceous inclusion formed at the centrosome that facilitates the degradation of excess amounts of protein (5).

While an overwhelming majority of PD is sporadic with unknown causes, 5-10% of PD is familial with a traceable genetic mutation (6). Six genes are linked with heritable, monogenic PD including *SNCA, LRRK2, Parkin, PINK1, DJ-1*, and *VPS35*(7). Out of these mutations, point mutations in the kinase Leucine-Rich Repeat Kinase 2 (LRRK2) are one of the three known autosomal dominant causes of PD (the others being VPS35 and *SNCA*). LRRK2-linked PD is also one of the most common causes of familial PD accounting for 5% of total familial PD cases and up to 40% of cases in familial PD in certain populations, including North African Berber and Ashkenazi Jewish patients (8). The penetrance for LRRK2 mutations varies with age and particular point mutations, ranging from 24% to almost 100% (9). Clinically, LRRK2-linked PD is similar to sporadic PD and has a late onset at around the age of 65 and slow progression (10).

Furthermore, polymorphism studies have revealed that SNP variations within the LRRK2 gene are risk factors for sporadic PD (11). This evidence suggests that LRRK2 may contribute to a disease pathway that is common to both sporadic and familial PD.

The LRRK2 protein is a large multidomain protein expressed ubiquitously at low levels throughout the body, with the highest expression in kidney, lung, and immune cells (Figure 1.1) (12). LRRK2 contains two enzymatic domains, a Roc (Ras of complex) GTPase domain and a serine-threonine kinase domain of the tyrosine kinase-like (TKL) family, linked together by a COR (C terminus of Roc) domain (13). In LRRK2's kinase domain, the activation loop contains a DYG motif which contains a tyrosine instead of the phenylalanine conserved in other kinases (14). The tyrosine hydroxyl decreases substrate accessibility to the activation loop and therefore decreases LRRK2 kinase activity (14). LRRK2 kinase domain's activity also requires activation of the Roc GTPase by GTP binding (15). Interaction between the LRRK2 kinase domain and Roc GTPase domain is mediated by the COR domain (16). In the catalytic portion of LRRK2, the Roc and COR domains are able to turn back towards the kinase domain, allowing the Roc domain and the kinase domain to interact (16).

Seven point mutations (G2019S, I2020T, R1441C/G/H, Y1699C, and N1437H) in LRRK2 have been identified to cause autosomal dominant PD (17). All identified LRRK2 point mutations lie in the catalytic region of LRRK2. The most common PD-driving variant, LRRK2 G2019S, lies in the kinase activation loop (18). Therefore, there is a significant amount of research into how LRRK2's disease-driving effects relate to LRRK2's kinase activity. *In vivo* studies and studies in cultured neurons demonstrated that mutant LRRK2's kinase activity is associated with its toxicity (19,20). These studies confirmed that expression of PD-mutant LRRK2 increases neuronal death (19,20). Furthermore, inhibiting the kinase activity can delay

cell death (19,20). There is also some evidence of increased LRRK2 activation in idiopathic PD (21). Based on this evidence, elevated LRRK2 kinase activity is strongly thought to contribute to the pathogenesis of PD.

LRRK2 may have significant endolysosmal function to maintain kidney and lung homeostasis. LRRK2 KO animals do not display any abnormality in the brain but have shown abnormalities in lung and kidney with enlarged lamellar bodies and secondary lysosomes (22). There is some evidence that lysosomal defects cause α-synuclein aggregation in LRRK2 KO mice (23). This suggests that LRRK2 may play a role in regulating protein turnover relevant to PD. Similarly, double knockout of LRRK1 and LRRK2 in mice causes impairment of the autophagy-lysosomal pathway and interestingly, these mice also show age-dependent dopaminergic neurodegeneration (24). Conversely, murine models with PD-related LRRK2 mutations do not consistently recapitulate human PD (25). These models do not demonstrate age-dependent dopaminergic neurodegeneration or α-synuclein pathology (25).

Due to its low expression level, visualizing endogenous LRRK2's subcellular localization is challenging. In overexpression systems, LRRK2 is mainly present in the cytoplasm (Figure 1.2 shows LRRK2 subcellular localization) (26). However, much evidence suggests that LRRK2 may play an important role at the membrane and the cytoskeleton. ~10-20% of LRRK2 forms membrane-associated dimers, which have increased kinase activity (26). Certain LRRK2 PD-driving point mutants (R1441C/G, Y1699C, I2020T, discussed in more detail below) appear to be localized around microtubule as filaments in overexpression; WT LRRK and G2019S LRRK also exhibit similar localization phenotype when treated with a kinase inhibitor (14).

At least some downstream substrates of LRRK2 have been reported. LRRK2 can autophosphorylate itself at its serine or threonine residues, especially at or close to the ROC

region (27). Out of the multiple autophosphorylation sites identified, Ser1292 seems to be particularly important (28). Several LRRK2 PD mutants are reported to cause increased autophosphorylation on Ser1292 including N1437H, R1441G/C, G2019S, and I2020T (28). LRRK2 phosphorylates a subset of Rab GTPases at the cell membrane (29). LRRK2 phosphorylates at least 14 Rab GTPases including Rab8, Rab10 and Rab29 on a conserved residue in their switch-II domains (30). These downstream substrates are also reported to show increased phosphorylation with LRRK2 PD-driving point mutations. Moreover, Rab29 can also activate LRRK2, at least when both proteins are overexpressed (31). Therefore, overactivation of LRRK2 might lead to hyperphosphorylation of downstream substrates, changing their function.

Although the mechanisms by which increased LRRK2 kinase activity causes neurodegeneration are unknown, decreasing LRRK2 kinase activity appears to be a plausible method to attempt to treatment for PD. Therefore, a series of potent LRRK2 kinase inhibitors have been developed including GNE-0877, MLi-2, and LRRK2-IN-1(32,33,34). These are type 1 kinase inhibitor that act as ATP-competitive inhibitors, binding to the active form of kinase and keeping the kinase in a closed conformation (35).

However, experiments reveal that kinase inhibition can cause toxicity to animal models. Both primate and mouse models have shown an accumulation of lamellar bodies in lung cells, indicating a defect in secretion or lysosomal function (33). This pulmonary change is phenotypically similar to LRRK2 knock out mice suggesting that the pathology is due to kinase inhibition and not an off-target effect. Therefore, it calls into question the safety of LRRK2 kinase inhibitors. While there is some evidence suggesting that the morphological change is reversible and does not influence pulmonary function, these studies are extremely short in duration (on the order of weeks) and there is no evidence about the long-term effects of kinase

inhibition in animal models (36). Moreover, in vitro experiments also showed that LRRK2 kinase treatment can lead to LRRK2 protein level changes (37,38).

In both endogenous and overexpression systems, Type 1 kinase inhibitor treatment can decrease LRRK2 levels (37,38). Kinase inhibition leads to dephosphorylation of LRRK2 in the serine sites (Ser910, Ser 935, Ser955, and Ser973) of a region designated the Regulatory Loop (amino acids 853-981). Dephosphorylation of these serines leads to ubiquitination of LRRK2 by an unknown E3 ligase followed by subsequent proteasomal degradation (38, 39). These results suggest that aside from altering LRRK2 kinase activity, LRRK2 protein abundance is also altered by Type 1 kinase inhibitor treatment. Thus, side effects from LRRK2 kinase inhibitors could be due to decreased LRRK2 levels rather than the direct effects of kinase inhibition. A growing body of evidence also suggests that LRRK2 protein levels may be relevant to PD. Researchers have reported that PD patients have more LRRK2 expression than healthy controls (40). Also, increased expression of mutated LRRK2 in neurons leads to neuronal death (41). Thus, in order to utilize LRRK2 as a target for PD treatment, we need a better understanding of the relation between LRRK2 protein abundance and LRRK2 kinase activity.

LRRK2 turnover in cells has been suggested to occur via multiple mechanisms. LRRK2 has been observed to be degraded through CMA (chaperone mediated autophagy) (42). CMA is a specialized component of the autophagy-lysosome pathway which ultimately degrades protein in the lysosome. CMA transports polypeptides with the KFERQ motif into the lumen of the lysosome by LAMP-2A and HSP8A (43). Interestingly, compared to WT LRRK2, LRRK2 G2019S is poorly degraded by this pathway (42). Additionally, studies of kinase inhibitor-mediated LRRK2 degradation pathway show that a large body of LRRK2 is degraded through the ubiquitin-proteasome system (UPS) (38,39). The UPS system uses a series of ubiquitin

ligases to tag substrates with ubiquitin causing the tagged protein to be degraded by the proteasome (44). The ubiquitination process features an E1 enzyme that activates ubiquitin, an E2 enzyme that accepts the activated ubiquitin and an E3 enzyme that transfers the activated ubiquitin to the protein (44). Multiple E3 ligases that interact with LRRK2 are known; the detailed interaction between specific E3 ubiquitin ligases and LRRK2 will be described in the next chapter.

Figures

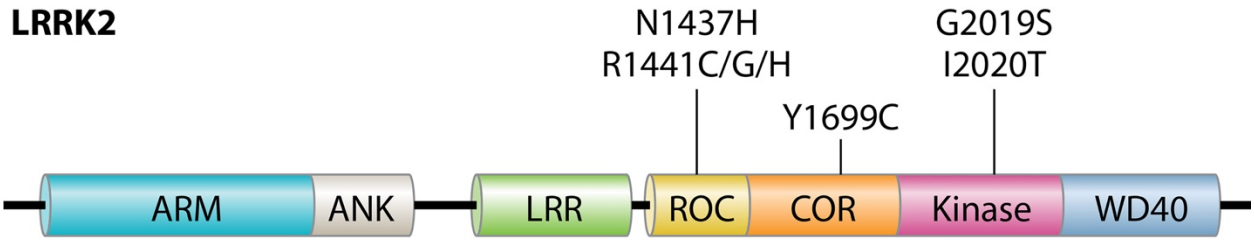

Figure 1.1: LRRK2 domain structure with seven known mutations driving autosomal dominant PD labelled. Adapted from Usmani *et al.* 2021(17)

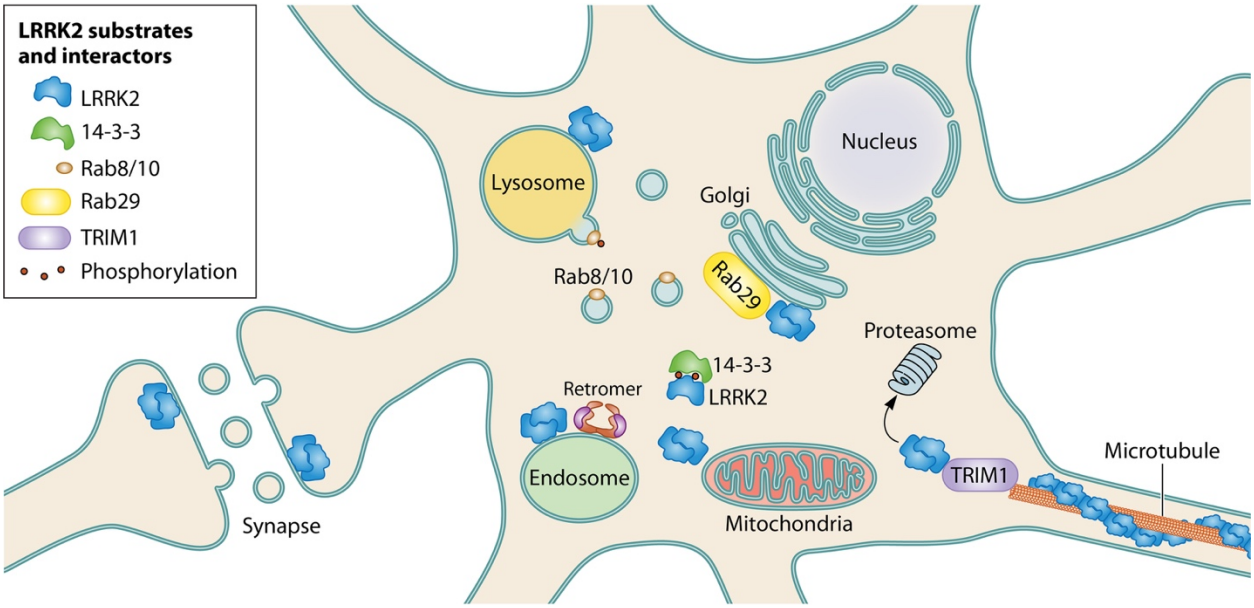

Figure 1.2: LRRK2 subcellular localization and key interacting proteins. LRRK2 is found primarily in the cytoplasm and interacts with 14-3-3 in a phosphorylation dependent manner. LRRK2 is also activated by Rab29 and can phosphorylate Rab8/10. LRRK2 also associates with the microtubule and this association is found to be mediated by TRIM1. Adapted from Usmani *et al.* 2021(17)

.CHAPTER 2 BIRC2 and PJA2 are not E3 ligases downstream of LRRK2 kinase inhibition

Introduction

As described in the previous chapter, cellular LRRK2 protein levels are heavily regulated by the ubiquitin-proteasome system. Therefore, identification of E3 ligases that interact with the ubiquitinated substrate, in this case LRRK2, is crucial for our understanding of LRRK2 degradation pathways. To this date, a variety of E3 ligases have been identified to interact with LRRK2, including CHIP1, WSB1, TRIM1, MARCH5, MULAN, and Skp1-Cullin1-F-box (45-50). C-terminus of Hsc70-interacting protein (CHIP1) is an HSP70 co-chaperone that preferentially interacts with many partially folded or misfolded proteins (45). CHIP1 appears to be important for degrading destabilized LRRK2, such as the protein from sporadic PD modest-risk allele LRRK2 G2385R (45).

WD repeat and SOCS box–containing 1 (WSB1) is an E3 ligase that does not promote LRRK2 proteasomal degradation (46). However, WSB1 is found to ubiquitinate LRRK2 via atypical K27 and K29 linkage which appear to cause LRRK2 aggregation (46). TRIM1 is a relatively newly identified LRRK2 interactor that regulates LRRK2 localization and mediates LRRK2 degradation (47). TRIM1 recruits LRRK2 to the microtubule cytoskeleton for ubiquitination and proteasomal degradation by binding the LRRK2 regulatory loop, a region between LRRK2's ANK and LRR domains (47). The association of LRRK2 and TRIM1 prevents upregulation of LRRK2 kinase activity by Rab29 in an E3-ligase-dependent manner and overexpression of TRIM1 rescues neurite outgrowth deficits caused by the LRRK2 G2019S mutant (48). LRRK2 is also reported to regulate the activities of E3 ubiquitin ligases MARCH5, MULAN, and Parkin via kinase-dependent protein-protein interactions (49). These interactions

are believed to mediate mitochondrial tethering by blocking PERK-mediated phosphorylation and activation of E3 ligase which stops ubiquitin-mediated protein degradation (49).

LRRK2 interacts with a component of the Skp1-Cullin1-F-box ubiquitin ligase complex, Fbxl18 (5). Phosphorylation of LRRK2 mediated by Protein Kinase C(PKC) allows Fbxl18 and LRRK2 interaction and promotes LRRK2 degradation via the ubiquitin-proteasome pathway (50). The selective degradation of phosphorylated LRRK2 may mitigate cell toxicity of PD mutant LRRK2 (50). All of this evidence suggests that LRRK2 is closely relevant to the proteasome-ubiquitin system.

As detailed in Chapter 1, kinase inhibitor treatment causes a decrease in LRRK2 protein level. Follow up investigation of LRRK2 kinase inhibition reveals that kinase inhibition leads to dephosphorylation of several serines in the LRRK2 Regulatory Loop (38,39). This dephosphorylation triggers ubiquitination of LRRK2 and proteasomal degradation of LRRK2 (38,39). Currently, the E3 ligase that ubiquitinates LRRK2 following kinase inhibition is unknown; TRIM1 and CHIP do not cause mediate degradation following kinase inhibition (38,39, 47). Therefore, identifying the E3 ligase that ubiquitinates LRRK2 following kinase inhibition can help us understand more about this pathway and potentially could advance treatment option for PD. From a CRISPRi genetic screen performed prior to this thesis, two new E3 ligases BIRC2 and PJA2, were identified to regulate LRRK2 protein levels after kinase inhibition. In this chapter, we aimed to confirm that two E3 ligases, BIRC2 and PJA2, cause LRRK2 degradation following Type 1 kinase inhibition.

Materials and Methods:

Cells

All mammalian cell lines were grown at 37℃ in a humidified atmosphere with 5% CO2. Doxycycline-inducible GFP-LRRK2 HEK-293T (51) cell lines were cultured in DMEM + 10% tetracycline-free FBS (Biowest, S1620) containing 10 μg/mL blasticidin S (RPI, B12150) and 100 μg/mL hygromycin B (Gibco, 10687010).

Plasmid and siRNA

SMARTpool siRNA with a mixture of multiple siRNA was ordered from Horizon for knockdown purposes. The siRNA used is as follows: siGENOME SMARTpool- Human PJA2 (M-006916-00-0005) and siGENOME SMARTpool- Human BIRC2 (M-004390-02-0005). PJA2 cDNA sequence was obtained by RNA extraction from HEK23T cells following rt-PCR. PJA2/MYC plasmid was constructed by cloning human PJA2 cDNA sequence into the pCMV-N2-6MYC-hMID2 (Addgene, 51035) plasmid.

Transfection, Knockdown and drug treatment

For overexpression of PJA2, doxycycline-inducible GFP-LRRK2 HEK-293T cell were transfected using Lipofectamine 2000 (Thermo Scientific, 11668030) per manufacturer's instructions at 3 μg. For PJA2 and BIRC2 knockdown, Doxycycline-inducible GFP-LRRK2 HEK-293T cells were transfected with PJA2 or BIRC2 siRNA with Amaxa Nucleofection. 0.5μM siRNA was electroporated into cells using the Amaxa Nucleofector II device and Cell Line Nucleofector Kit V (Lonza Bioscience, VCA-1003). The cells were electroporated by preprogramed HEK-293T cell program (program A-023). The cells were transfected for 8 hours

before drug treatment for overexpression and for 24 hours for knockdown. Success of transfection and knockdown was validated with immunoblot or qPCR. LRRK2 expression was induced with 5 ng/ml doxycycline (20592-13-9). Kinase activity was inhibited with 2μM/ml MLi-2(Abcam ab254528) for 16 hours to 24 hours. Bortezomib (179324-69-7) was used at 1 μM for 24 hours.

Flow Cytometry

GFP-LRRK2 levels were measured in doxycycline-inducible cell lines on a BD FACSCanto™ II cell analyzer. On the day of analysis, cells were trypsinized, pelleted, and washed. Cell pellets were than resuspended in 2% FBS PBS. GFP intensity was measured using a 488-nm laser for excitation and a detector with a 530/30 BP filter and 502 LP mirror. Only live, single cells, as determined by forward and side scatter, were analyzed. Live cells were selected with 7-AAD dye. Single cells were selected based on forward and side scatter. Only live and single cells were selected for data analysis. Flow cytometry data was analyzed using FlowJo software.

Western blotting

Cell pellets were lysed for 30 min at 4°C with end-over-end mixing in cold lysis buffer [50 mM tris pH 7.5 | 150 mM NaCl | 1 mM EDTA | 0.5% NP-40 | 1x protease (Roche, 11836170001) and phosphatase (Roche, 04906845001) inhibitors]. Protein samples (50μg) were electrophoresed using NuPAGE 4-12% Bis Tris (Invitrogen, NP0321) or 3-8% Tris Acetate (Invitrogen, EA0375) polyacrylamide gels. Proteins were transferred from gels onto PVDF membrane (EMD Millipore, IPFL00010) using the Genscript eBlot L1 wet transfer system (cat#

L00686). Membranes were blocked using LI-COR Intercept Blocking Buffer (cat# 927-60001). All primary antibodies were used at 1:1000 dilution. Primary antibodies used is as follows: LRRK2 C41-2 (Abcam, 133474), rabbit PJA2 (Cell Signaling, 40180S), rabbit BIRC2 (Abcam, ab108361), mouse beta-actin (Cell Signaling, 3700S), mouse beta-tubulin (Cell Signaling, 86298S), mouse MYC (Sigma, M4439). Primary antibodies were incubated overnight at 4°C. Both secondary antibodies (IRDye® 800CW or 680RD Goat anti-Mouse or Goat anti-Rabbit IgG, LI-COR) were used at 1:10,000 dilution. Secondary antibodies were incubated at room temperature for 30-50mins. All imaging was performed using a LI-COR Odyssey® CLx imaging system. Quantification of individual western band was obtained on ImageStudioLite.

qPCR

RNA was extracted from cells with NucleoSpin® RNA Plus kit (740990.10) per manufacture protocol. After RNA concentration quantification with nanodrop, samples were normalized to a concentration of 100 ng/μL. CDNA was synthesized by RT-qPCR with High-Capacity cDNA Reverse Transcription Kits (Applied Biosystem, 4368814). Q-PCR sample were prepared in triplicate at 10μl reaction volume with 1x TaqMan Universal PCR Mastermix (Thermo Scientific, 4352042) and probe against protein of interest at 1:10 dilution. TaqMan probe for Q-PCR was as follows: PJA2 (Hs01122981_m1),18s (Hs99999901_s1). QPCR was performed on StepOnePlus machine (Applied Biosystem) with Comparative ΔΔCT analysis. Protein CT was normalized to control 18S to visualize changes in protein quantities.

Results

Type 1 kinase inhibitors cause LRRK2 turnover through the proteasome while Type 2 kinase inhibitors do not

Given LRRK's low endogenous level, the first goal for this project was to find a system that we can use to reliably measure LRRK2 abundance. With a doxycycline-inducible GFP-LRRK2 HEK-293T cells line, we were able to monitor GFP-LRRK2 expression with doxycycline ("dox") induction by both western blotting and flow cytometry (Figure 2.1a). With dox induction at different time points, we were able to show that the normalized GFP-LRRK2 signal change measured by flow cytometry was indeed proportional to the LRRK2 signal measured by immunoblots (Figure 2.1b).

Furthermore, we confirmed findings from previous studies that kinase inhibition can lead to LRRK2 degradation (38,39). We found that in the doxycycline-inducible GFP-LRRK2 cell line, treatment with MLi-2 at 2μM for 24 hours led to a 56% decrease in LRRK2 abundance (Figure 2.1c, d, e). This finding was reproducible with both western blotting and flow cytometry. Moreover, we confirmed that LRRK2 turnover after kinase inhibition is mediated by the proteasome. We found that MLi-2 co-treatment with bortezomib, a proteasome inhibitor, at 1μM for 24 hours rescued LRRK2 protein levels as measured by both western blotting and flow cytometry (Figure 2.1c, d, e). This suggested that LRRK2 turnover following MLi-2 treatment is mediated by one or multiple ubiquitin E3 ligases.

Type 1 kinase inhibitors function by blocking LRRK2 at an inactive form. A new generation of kinase inhibitors, type 2 kinase inhibitors, have being developed to lock the kinase in its active form. Compared to a type 1 kinase inhibitor, in this case MLi-2 treatment, the type 2

kinase inhibitor (rebastinib) did not cause change in LRRK2 abundance as measured by flow cytometry (Figure 2.1f).

LRRK2 turnover is by an unknown E3 ligase

Previous work performed by a graduate student in Scott Oakes' lab at UCSF used the tet-GFP-LRRK2 system and a CRISPRi screen to identify candidate E3 ligases responsible for LRRK2 turnover following MLi-2 inhibition versus control conditions. The study transduced cells with a sgRNA library composed of 3,093 stress and proteostasis genes, including nearly all of the estimated 600-700 human E3 ubiquitin ligases. Afterward, the cells were treated with the kinase inhibitor, MLi-2. The cells were then sorted by flow cytometry and the cells with the highest GFP-LRRK2 signal were then collected for NGS sequencing. The sequencing results were then mapped to sgRNA reference sequences to determine the count for each individual sgRNA. The counts were then used to identify which gene was enriched in the cell population.

Some major findings of the study were 1) the list of genes that were enriched in the LRRK2 kinase inhibitor treated condition versus the control condition differed. This result suggested that LRKK2 turnover after kinase inhibition involves a unique pathway different from basal LRRK2 degradation pathways. 2) Several E3 ligases were identified as significantly enriched after kinase inhibitor treatment. After further validation, sgRNA knockdown of two E3 ligases PJA2 and Birc2 showed increased LRRK2 levels. Here, we tried to first verify these finding with downregulation and overexpression of PJA2.

First, we tried to rescue LRRK2 turnover with knockdown of PJA2. We introduced a pool of 4 PJA2 siRNAs or control siRNA into the Doxycycline-inducible GFP-LRRK2 cells by electroporation. Afterwards, the cells were induced for 24 hours with 5ng of doxycycline to

induce LRRK2, dox was removed, and the cells were treated with 2μM MLi-2 for 16 hours. The cells were harvested and subjected to flow cytometry, qPCR, or immunoblot. LRRK2 levels were measured with western blotting or flow cytometry while PJA2 protein was measured with qPCR (we were unable to identify an antibody that reproducibly measured endogenous Pja2 on immunoblot). Knockdown of PJA2 with siRNA did not significantly rescue LRRK2 levels (Figure 2.2d). This result was confirmed with both western blotting and flow cytometry (Figure 2.2b, c).

Moreover, we also tested if overexpression of PJA2 can decrease LRRK2 levels. We transfected the Dox-HEK cell line with MYC tagged PJA2 plasmid and repeated the same experimental setup in an overexpression system. The transfection was verified by using an antibody that identifies the MYC tag (Figure 2.2e). Overexpression of PJA2 also did not cause further decrease of LRRK2 level on a western blot and Flow cytometric histograms (Figure 2.2e, f, g). Thus, both knockdown and overexpression studies indicated that PJA2 has no effect on LRRK2 turnover.

Next, we moved on to the second possible candidate BIRC2 and attempted to rescue LRRK2 turnover by BIRC2 knockdown. We introduced either a pool of 4 BIRC2 siRNA or a control scramble siRNA into the Doxycycline-inducible GFP-LRRK2 cells by electroporation. After exposing the cells to siRNA for 24 hours, the cells were induced for 24 hours with 5ng of doxycycline. Dox was removed and cells were treated with 2μM mLi-2 for 24 hours before harvesting. Harvested cells were subjected to flow cytometry or immunoblot. LRRK2 levels were measured with both western blotting and flow cytometry while BIRC2 knockdown was verified with immunoblot. Knockdown of BIRC2 with siRNA did not significantly rescue LRRK2 levels (Figure 2.3a, c, d). This result was confirmed with both western blotting and flow

cytometry. These results indicated that BIRC2 also does not appear to affect LRRK2 turnover following MLi-2 treatment. Therefore, an unknown E3 ligase not identified in this original screen appears to be responsible for LRRK2 turnover following MLi-2 treatment.

Discussion

Highly selective type 1 kinase inhibitors such as MLi-2 have been developed as a potential PD treatment (35). However, research suggested that type 1 LRRK2 kinase inhibitor treatment can lead to LRRK2 turnover (38,39). Either kinase inhibition or decreased LRRK2 protein levels appears to be potentially toxic to peripheral organs causing defects in secretion or lysosomal function in lung cells (33). These results call into question the safety of such drugs in humans. Therefore, in order target LRRK2 kinase activity, we need a better understanding of the relationship between inhibition of LRRK2 kinase activity and LRRK2's degradation.

The relationship between LRRK2's kinase activity and its protein level is not well understood. A significant body of research relates LRRK2 toxicity to its kinase activity but there is a growing evidence suggesting that increased LRRK2 protein levels may also be toxic (19,20,40,41). LRRK2 protein levels have been shown to be dependent on its kinase activity (22). However, there is also evidence suggesting that increased expression of mutated LRRK2 in neurons rather than kinase activity alone correlates with neuronal death (41). In order to better understand the relationship between LRRK2 kinase inhibition and degradation, identification of the E3 ligase responsible for LRRK2 ubiquitination following kinase inhibition is crucial. In a previous CRISPRi screen, BIRC2 and PJA2 were identified by the Oakes lab as two E3 ligases responsible for LRRK2 turnover after kinase inhibition. However, this section shows that we were not able to replicate the result. Neither downregulation nor overexpression affected LRRK2 abundance in cells.

After a more thorough investigation of the original screen data, we found that the data generated appeared to be suboptimal for a number of reasons. First, there appeared to be significant contamination of particular single guides in the sgRNA library rather than a uniform

or normal distribution of guides as would be expected. Given the large numbers of guides within a single sgRNA library, the relative level of a single guide is considerably lower than the same guide when prepped individually. Therefore, CRISPRi screening can be susceptible to contamination of individual DNA plasmid. Looking at the actual screen data, the reads for guides have a right skewed distribution compared to the expected normal distribution. The right skew shows that some guides are overrepresented in the cell population collected while others are not recorded. Therefore, this result suggests that the data may have also left out many actual targets.

Additionally, in retrospect, it was surprising how few genes replicated between the control condition (i.e., regulating LRRK2 under basal turnover conditions) and MLi-2 treatment. While LRRK2 could be under different regulation with or without pharmacological intervention, it is unlikely that the pathways do not overlap at all. Given these indications that the previous screen was suboptimal, a proximal next step is to rescreen for new candidates potentially responsible for LRRK2 turnover. Although this work failed to replicate the result of the initial screen, we did verify that LRRK2 degradation following kinase inhibition occurs via the ubiquitin-proteasome system. Considering the association of LRRK2 and the ubiquitin-proteasome system, the next step was to conduct the next screen in a more precise way targeting only the ubiquitin-proteasome system as described in Chapter 3. In this way, we predicted we would be able to narrow down the range of the library and do a more complete data analysis.

Lastly, MLi-2 is a type 1 kinase inhibitor, which competes with ATP binding to inhibit LRRK activity. LRRK2 type 2 kinase inhibitors are now being developed, which function by a different mechanism. These type of kinase inhibitors bind to the inactive form of the kinase and lock the kinase in the inactive form (35). In this section, we showed that rebastinib, a type 2 kinase inhibitor, does not result in LRRK2 degradation after treatment. This result suggests that

LRRK2 degradation after kinase inhibition may be LRRK2 conformation dependent. However, rebastinib was not developed as a selective LRRK2 kinase inhibitor and these are still in development. While our work suggested that type 2 LRRK2 selective kinase inhibitors should not mediate LRRK2 degradation, more research will be needed to define this once these inhibitors exist.

Figures

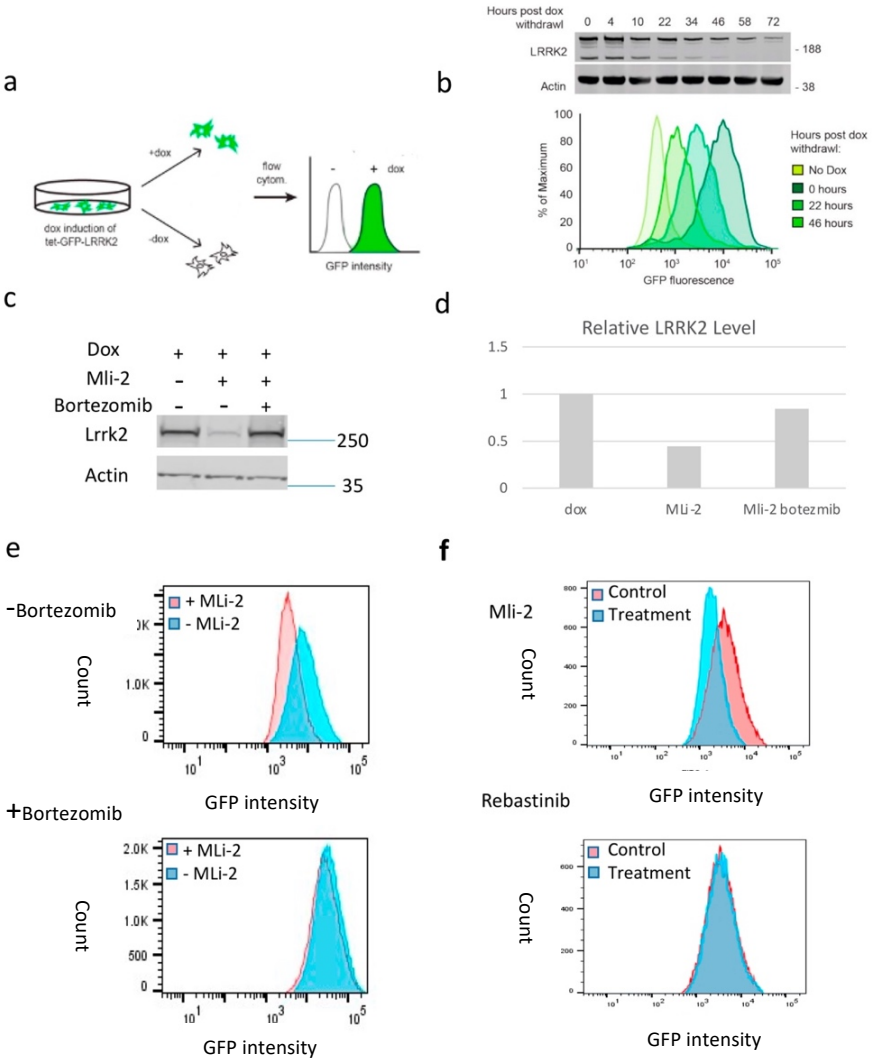

Figure 2.1: Overview of LRRK2 quantification in Doxycycline-inducible GFP-LRRK2 HEK-293T cells and LRRK2 proteasomal degradation following kinase inhibition. a) Schematic of flow cytometric assay using fluorescence to measure GFP-LRRK2 turnover. Doxycycline-inducible GFP-LRRK2 HEK-293T cells are induced for 18 to 24 hrs, transfected and doxycycline simultaneously withdrawn, and GFP fluorescence measured 18 to 24 hrs later. b) Immunoblot showing LRRK2 levels relative to actin after doxycycline induction for a variable time period and flow cytometric histograms of median GFP fluorescence from the same samples. c) Immunoblot showing LRRK2 levels change relative to actin after doxycycline treatment (doxycycline-induced for 24 hrs) following kinase inhibitor (mLi-2 treatment for 24 hrs) or kinase inhibitor (mLi-2) and proteasomal inhibitor (bortezomib) co-treatment (for 24 hrs). d) Quantification of LRRK2 levels change in c) e) Flow cytometric histogram showing LRRK2 level changes after doxycycline treatment (doxycycline-induced for 24 hrs) following kinase inhibitor (mLi-2 treatment for 24 hrs) or kinase inhibitor (mLi-2) and proteasomal inhibitor (bortezomib) co-treatment (for 24 hrs).f) Flow cytometry histogram showing LRRK2 level change after doxycycline treatment(doxycycline induced for 24 hrs) following kinase inhibition(for 24 hrs) by either type one kinase inhibitor (mLi-2) or type two kinase inhibitor (rebastinib). Panel B is from Ref 47.

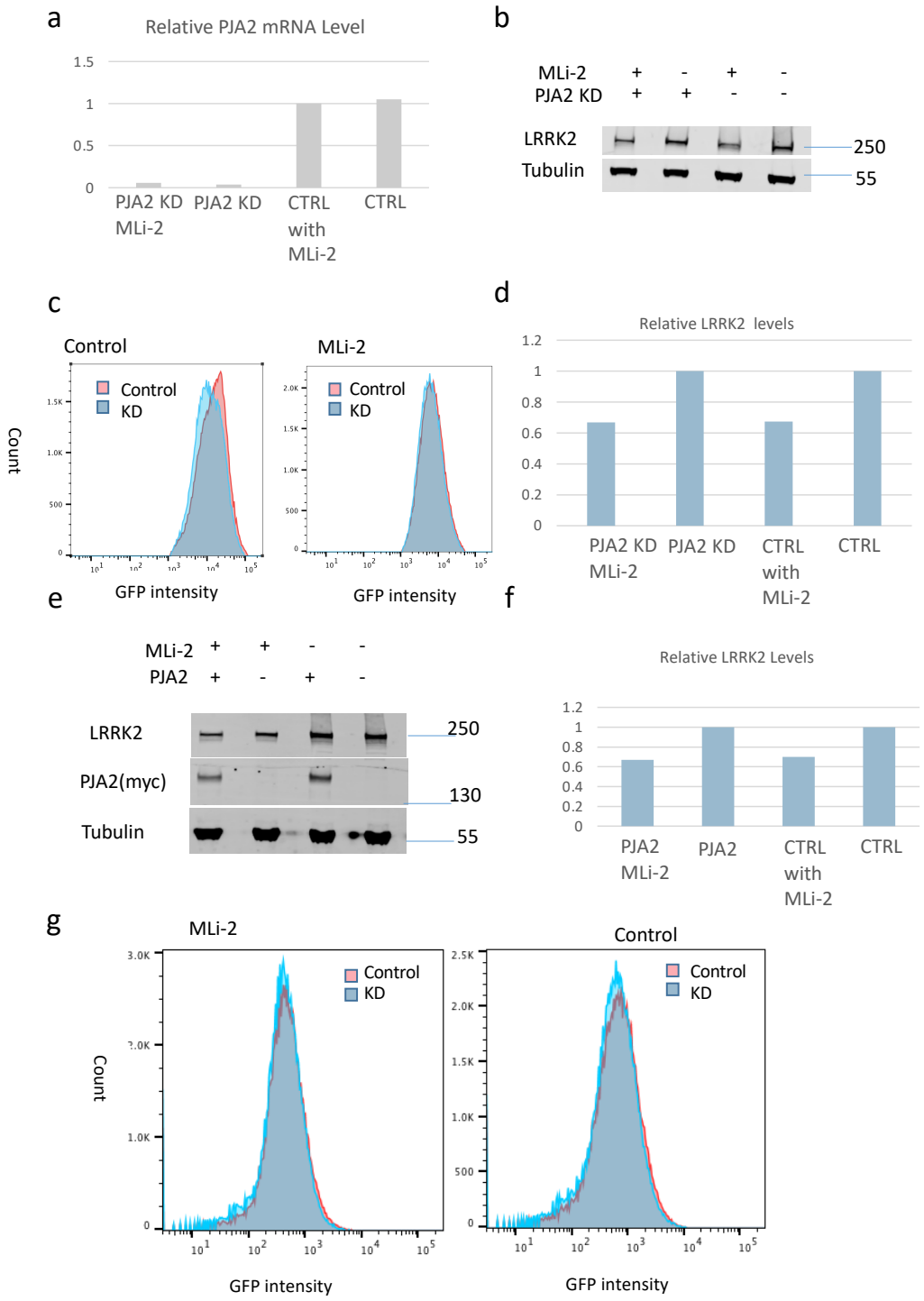

Figure 2.2: Changes in LRRK2 expression with PJA2 knockdown and overexpression a) Quantification of PJA2 levels change by q-PCR b) Immunoblot showing LRRK2 levels change relative to tubulin with PJA2 knockdowns and kinase inhibitor treatment (mLi-2 treatment for 16 hrs; Representative experiments shown, n=8 for PJA2 KD).c) Flow cytometric histograms showing LRRK2 level changes with PJA2 knockdowns and kinase inhibitor treatment (mLi-2 treatment for 16 hrs). d) Quantification of PJA2 levels change in c). e) Immunoblot showing effect of PJA2 overexpression on LRRK2 level relative to tubulin in the presence and absence of kinase inhibitor treatment (mLi-2 treatment for 16 hrs). Representative experiments shown, n=2 for PJA2 overexpression. f) Quantification of LRRK2 levels change in e). g) Flow cytometric histograms showing LRRK2 level changes with PJA2 transfection and kinase inhibitor treatment (mLi-2 treatment for 16 hrs)

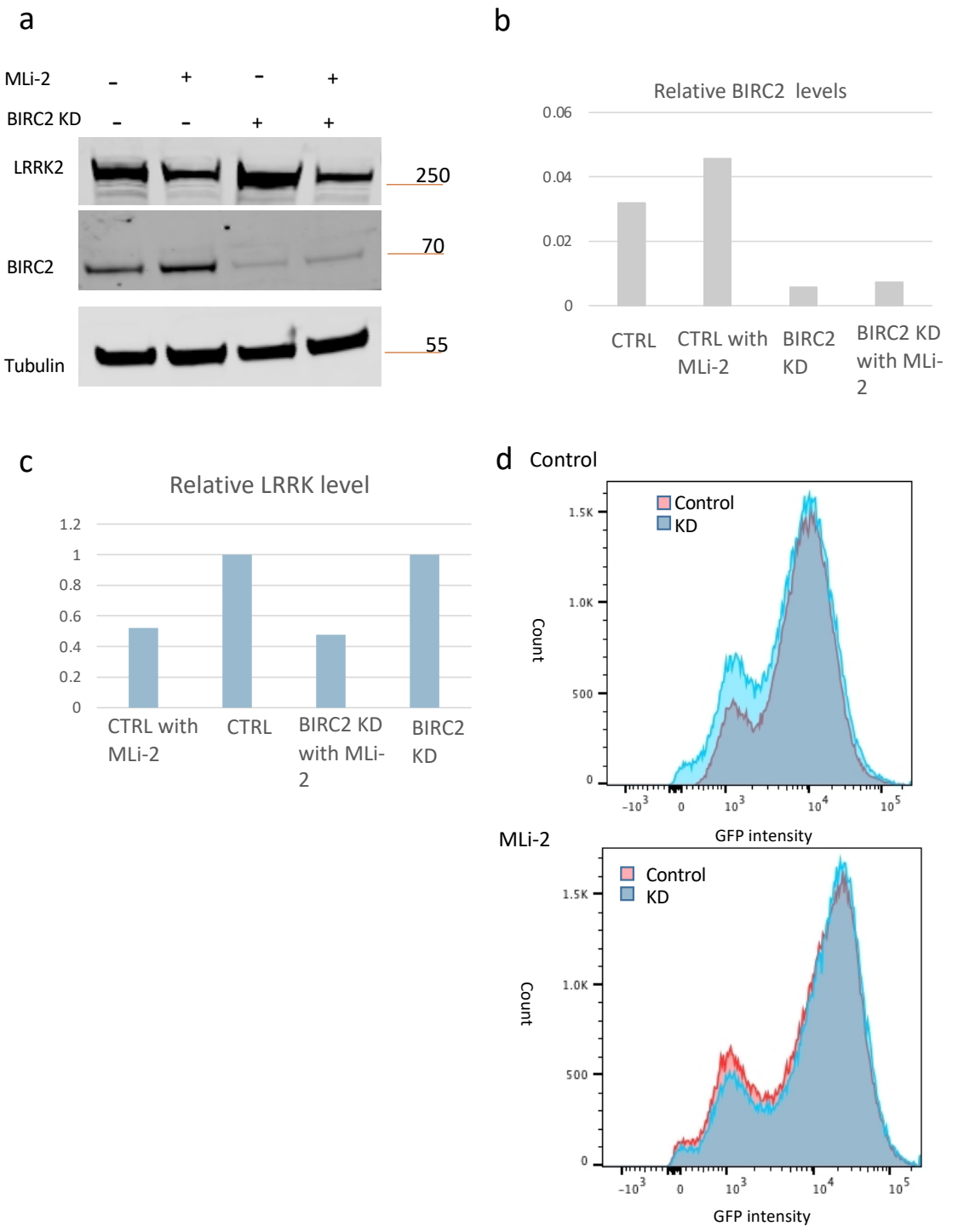

Figure 2.3: Changes in LRRK2 expression with BIRC2 knockdown. A) Immunoblot showing LRRK2 levels change and BIRC2 level change relative to tubulin with BIRC2 knockdowns and kinase inhibitor treatment (mLi-2 treatment for 24 hours). Representative experiments shown, n=8 for BIRC2 KD b) Quantification of BIRC2 level change in a). c) Quantification of LRRK2 level change in a). d) Flow cytometric histograms showing LRRK2 level changes with BIRC2 knockdowns and kinase inhibitor treatment (mLi-2 treatment for 24 hours).

CHAPTER 3 CRISPRi screening to identify new LRRK2 regulatory pathways

Introduction:

The ubiquitin-proteasome system (UPS) is a key regulator of protein homeostasis by regulating protein turnover through proteasomal degradation. As discussed in Chapter 1 and Chapter 2, the UPS appears to be the key driver of LRRK2 protein degradation in vivo. Within the ubiquitin-proteasome system, protein post-translation modification with ubiquitin-like proteins can also influence proteostasis. These modifications, such as SUMOylation and neddylation, usually do not directly regulate protein turnover but can be essential for protein stability, subcellular localization and protein-protein interactions (52, 53). Similar to ubiquitination, both SUMOylation and neddylation utilize E1, E2 and E3 enzymes (52, 53). For SUMOylation, a small molecule SUMO is conjugated to the lysine residue of a substrate (54). Research has identified two E1 enzymes SAE1/2 (also known as AOS1 and Uba2, respectively), one E2 enzyme UBC9, and multiple E3 ligases characterized into five families (the SP-RING domain family, the TRIM superfamily, non-canonical ligases, ligase-like factors, and the other SUMO E3 ligases) (54). For neddylation, modified NEDD8 protein is conjugated to the substrate protein (55). A heterodimer E1 enzyme NAE, (formed by NAE1 and UBA3), two E2 enzymes Ubc12 (Ube2M) and Ube2F, and a variety of E3 ligase substrates, including a series of cullin family proteins, have been identified as part of the neddylation pathway (55).

Many researchers have also reported that neddylation and SUMOylation may play a role in neurodegenerative disease. For example, PD-associated parkin and PINK1 are modified by neddylation and neddylation increases parkin E3 ligase activity while stabilizing PINK1(56). SUMOylation has been reported to prevent α-synuclein aggregation and DA neuron degeneration

(57). These ubiquitination-like modifications could also be important in regulating LRRK2 PD pathogenesis.

One way to study the function of a gene is to repress the gene's expression through knockdown and evaluate the phenotype following knockdown. One way to generate these knockdowns is through CRISPR interference (CRISPRi) (58). CRISPRi uses an endonuclease-inactive dCas9-RNA complex that can target a specific sequence of a gene with the help of a short RNA sequence (sgRNA) that base pairs to a specific region of the original sequence but cannot cut the sequence (58). Fusing the dCAS9 protein with a repressor such as KRAB (Krüppel Associated Box), we can target the repressor to specific locations within the genome, thus decreasing gene expression (58). To systematically understand the function of proteins within a large pathway, genetic screening in cultured cells is a powerful tool. Combining a genetic screening strategy and CRISPRi leads to a technique in which pooled sgRNA libraries targeting a large number of genes can be used to identify genes important in a given pathway (59).

For this chapter, we conducted a CRISPRi screen using a novel ubiquitin-proteasome system (UPS) sgRNA library to identify proteins that regulate LRRK2 turnover within the UPS. We screened in the presence and absence of the LRRK2 inhibitor MLi-2. This screen identified the ubiquitination-like modification systems neddylation and SUMOylation as novel candidate pathways regulating LRRK2 protein degradation.

Methods

Cells

All mammalian cell lines were grown at 37°C in a humidified atmosphere with 5% CO2. Doxycycline-inducible GFP-LRRK2 HEK-293T (7) cell lines were cultured in DMEM + 10% tetracycline-free FBS (Biowest, S1620) containing 10 μg/mL blasticidin S (RPI, B12150) and 100 μg/mL hygromycin B (Gibco, 10687010).

Drug treatment

LRRK2 expression was induced with 5 ng/ml doxycycline (20592-13-9). Kinase activity was inhibited with 0.5-2μM/ml MLi-2 (Abcam, ab254528) for 24 hrs prior to harvesting.

Flow Cytometry

GFP-LRRK2 levels were measured in doxycycline-inducible cell lines on a BD FACSCanto™ II cell analyzer. On the day of analysis, cells were trypsinized, pelleted, and washed. Cell pellets were then resuspended in 2% FBS PBS. GFP intensity was measured using a 488-nm laser for excitation and a detector with a 530/30 BP filter and 502 LP mirror. Only live, single cells, as determined by forward and side scatter, were analyzed. Flow cytometry data was analyzed using FlowJo software.

Western blotting

Cell pellets were lysed for 30 min at 4°C with end-over-end mixing in cold lysis buffer [50 mM tris pH 7.5 | 150 mM NaCl | 1 mM EDTA | 0.5% NP-40 | 1x protease (Roche, 11836170001) and phosphatase (Roche, 04906845001) inhibitors]. Protein samples (5μg) were electrophoresed

using NuPAGE 4-12% Bis Tris (Invitrogen, NP0321) or 3-8% Tris Acetate (Invitrogen, EA0375) polyacrylamide gels. Proteins were transferred from gels onto PVDF membrane (EMD Millipore, IPFL00010) using the Genscript eBlot L1 wet transfer system (cat# L00686). Membranes were blocked using LI-COR Intercept Blocking Buffer (cat# 927-60001). All primary antibodies were used at 1:1000 dilution. Primary antibodies used is as follows: rabbit LRRK2 C41-2(Abcam, 133474), rabbit PSMD4(Cell signaling, 12441), rabbit SAE1(Cell signaling, 13585), rabbit NEDD8(Cell Signaling, 2745), rabbit PIAS2(Abcam,126601), rabbit RBX1(Cell signaling, 11922), mouse beta-actin (Cell signaling, 3700S). Primary antibodies were incubated overnight at 4°C. For fluorescent detection of western blots, both secondary antibodies (IRDye® 800CW or 680RD Goat anti-Mouse or Goat anti-Rabbit IgG, LI-COR) were used at 1:10,000 dilution. For chemiluminescent detection of western blots, donkey anti-rabbit (Jackson ImmunoResearch, 711-035-152) secondary antibodies were used at 1:10,000 dilution. Secondary antibodies were incubated at room temperature for 30-50mins. Fluorescent detection was performed using a LI-COR Odyssey® CLx imaging system. Quantification of individual western band were obtained on ImageStudioLite. Chemiluminescent detection was carried out with SuperSignal West Pico PLUS (Thermo Scientific, cat# 34579) reagent and blots were imaged using an Azure Biosystems c300 Imager.

Plasmid and cloning

Lentivirus packing plasmid pMD2.G (addgene, 12259) and psPAX2 (addgene, 12260) plasmid was a gift from the Bui lab. Lentivirus transfer plasmid control was a gift from the Kampmann lab (addgene, 127965). Lentivirus transfer plasmid for individual sgRNA was created by cloning

individual oligos into the transfer control plasmid. Individual sgRNA oligos were synthesized based on predicted sequences from supplementary file 3 in Horlbeck et al (61).

Generation of sgRNA lentiviral vector

Lentiviral vector was generated by transfecting in pMD2, psASX2 and lentivirus transfer plasmid with Lipofectamine 2000 at 1:2:4 ratio. Lentivirus expressing the sgRNA was harvested 48 hrs after transfection. The supernatant was passed through a .44μm filter (Millipore Sigma, SLHV033RB) and concentrated with lentiX concentrator (Takara bio, 631232). Lentivirus was used for cell transduction immediately or frozen at -80°C for further use.

Knockdown with single sgRNA

Lentivirus was transduced with 5μg/ml of polybrene transfection reagent (Fisher Scientific, NC9200896). The lentivirus polybrene mixture was removed 24 hrs after transduction. Puromycin (Omega Scientific, 58-58-2) was added at 1μg/ml for selecting sgRNA positive cells 48 hrs after transduction for 48 hrs-72hrs. The puromycin was then removed and the cells were treated with different drug treatments. Knockdown of individual sgRNA was validated by western blotting.

CRISPRi screening

CRISPRi screening was done at the Kampmann lab at UCSF. The UPS sgRNA libraries with top 5 sgRNA per gene were generated by transfection into HEK293T cells with 3rd generation lentiviral packaging plasmid mix (1:1:1 of the three plasmids) using TransIT®-Lenti (MIR 6600) Transfection Reagent. The virus was harvested 48 hrs after transfection with the method

described above in generation of single sgRNA lentiviral vector. Doxycycline-inducible GFP-LRRK2 with dCas9-BFP cells were plated 24hr prior to transduction. Cells were transduced with lentiviral preparations of the UPS library and selected with puromycin(2μg/ml) for 3-4days. Afterward, selection was removed and all plated cells were incubated with regular media for one day. Cells were then reseeded and induced with 5 ng/mL doxycycline. 24 hrs after induction, doxycycline was washed off and half of the plated cells were treated with 2 μM MLi-2. 24 hrs after treatment, the cells were harvested and sorted. Live, single, sgRNA+ cells (as determined by BFP fluorescence) were sorted by GFP signal. The top 30% and bottom 30% of GFP-LRRK2 expressing cells from each treatment group were collected for deep sequencing.

To prepare samples for sequencing, genomic DNA for sorted samples was extracted with the NucleoSpin Blood L kit (Macherey-Nagel). PCR was performed to amplify the sgRNA and add adapter/barcodes to the end of the sgRNA. Amplified PCR products were purified with SPRI beads. The purified samples were than quantified and pooled for sequencing.

Results

CRISPRi screen against UPS genes identifies several candidate regulators of LRRK2 levels

To generate a system that expresses the CRISPRi machinery, we transduced dox-GFP-LRRK HEK293T cells described in the previous chapter with an insulated BFP-dCAS9 construct (Figure 3.1a) to generate a stable cell line. To validate CRISPRi activity in these cells, we transduced them with an sgRNA targeting the transferrin receptor gene (TFRC) and showed that knockdown of TFRC is robust in the LRRK2 overexpression line (Figure 3.1b).

We then used this line to identify potential LRRK2 regulators in a CRISPRi genetic screen. To focus on LRRK2 turnover regulators, we used a CRISPRi sgRNA library specific to the UPS system that targets 1,693 genes within the UPS system with at least five independent sgRNAs per gene. Following lentiviral transduction and puromycin selection, cells were dox-induced, then dox was removed and cells were treated with MLi-2 or left untreated. After the drug treatment, the top and bottom 30% of GFP-LRRK2-expressing cells were identified and collected by FACS for NGS (next generation sequencing). To reduce the possibility of false positives, each screen +/- kinase inhibitor was done twice. Therefore, we ended up with 4 screen results: Screen1+/- MLi-2, and Screen2 +/- MLi-2. After obtaining the NGS sequencing results, the reads were analyzed by the MAGeCK pipeline developed by the Kampmann lab (60). Through this pipeline, we were able to assign knockdown phenotype scores and p-values for each sgRNA. From this, we calculated the strength of the knockdown, defined as the product of the knockdown phenotype score and the -log of the p-value. Based on the distribution of this product, we generated a cut-off and returned a list of hits of genes significantly enriched in either the top or bottom 30% of LRRK2-expressing cells (Figure 3.2a).

Following the construction of this list of candidate genes, we proceeded to evaluate the effectiveness of the screen. We transduced the cells with sgRNA against one top hit, PSMD4, and one bottom hit, CBLL1, which were both present as significant hits in all four screens. Flow cytometry analysis validated that knockdown of these individual genes moved the LRRK2-GFP protein levels in the expected direction, with PSMD4 knockdown causing an increase in LRRK2 levels while CBLL1 knockdown causing a decrease in LRRK2 levels (Figure 3.3).

SUMOylation and neddylation pathways may regulate LRRK2 protein levels.

Further examination of the top hits identified in the screens (i.e., genes that when knocked down led to an increase in LRRK2 protein levels) revealed that genes associated with two ubiquitin-like pathways, SUMOylation and neddylation, were enriched. Three of the top 10 ranked genes from all 4 screens are critical components of the SUMOylation pathway, including the heterodimer E1 complex SAE1/UBA2 (Figure 3.2 b). We also found 3 genes in the top 10 ranked genes are components of the neddylation pathway, including Nedd8, the ubiquitin-like protein that is transferred to substrates (Figure 3.2 b). Next, we evaluated the screens with and without MLi-2 treatment separately to determine whether proteins specific to either neddylation or SUMOylation were enriched in an MLi-2-dependent manner. Interestingly, genes involved in SUMOylation ranked higher in the untreated condition while genes involved in neddylation ranked higher in the MLi-2-treated condition (Figure 3.4). Therefore, this suggests that LRRK2 may be regulated by both SUMOylation and neddylation with neddylation being the more MLi-2 relevant pathway.

In order to confirm this possibility, we generated individual guides to test candidate genes in each pathway. For SUMOylation, we generated sgRNAs against SAE1. LRRK2 levels

increased with individual SAE1 sgRNA knockdown. This result was observed by both flow cytometry and western blotting (Figure 3.5). However, concurrent treatment with MLi-2 showed no increase in LRRK2 levels (Figure 3.5). For neddylation, we transduced cells with UBA3 sgRNA. LRRK2 levels also increased with UBA3 knockdown (Figure 3.6). Moreover, concurrent treatment with MLi-2 also increased LRRK2 levels (Figure 3.6).

The E3 ligases PIAS2 and RBX1 may interact with LRRK2

Similar to the traditional UPS system, both SUMOylation and neddylation contain an E3 ligase that interacts directly with the SUMOylated or neddylated substrate (53). Therefore, identification of an E3 ligase is essential for our understanding of these pathways and may also prove to be a therapeutic target.

Examining the screen results for candidate E3 ligases, the highest-ranked E3 ligase gene involved in neddylation was RBX1, which was significant in both screens with MLi-2. For SUMOylation, the highest ranked E3 ligase was PIAS2, which was significant in both screens without MLi-2. The fact that these two proteins were exclusively enriched in screens with different treatment conditions suggests that each may regulate LRRK2 turnover under particular conditions. Therefore, we transduced cells with individual sgRNAs targeting RBX1 and PIAS2 to test whether knockdown of these two genes affect LRRK2 levels.

For RBX1 knockdown, LRRK2 levels increased by more than two-fold for both the non-kinase inhibitor treated group and the MLi-2 treated group (Figure 3.7). These results suggest that loss of RBX1 significantly decreased LRRK2 turnover to increase LRRK2 protein levels. For PIAS2 knockdown, LRRK2 levels decreased by roughly 50% for both the non-kinase inhibitor treated group and the MLi-2 treated group (Figure 3.8). This result is contradictory to

the screening result as decrease PIAS2 level increased LRRK2 degradation instead of decreasing it. Therefore, RBX1 can be a negative regulator for LRRK2 turnover but PIAS2, surprisingly, may be a positive regulator for LRRK2 turnover.

Discussion

LRRK2 protein abundance may be a driver for LRRK2-relevant PD (41). Studies have shown that neuronal death increases with increasing LRRK2 protein levels (41). However, the mechanism by which this may occur is not well understood and basal protein degradation pathways for LRRK2 are not fully defined. Moreover, LRRK2 kinase inhibition can drive LRRK2 proteasomal degradation; however, the pathways by which this occurs are also unidentified. Therefore, defining LRRK2 protein degradation pathways might offer valuable insights into understanding PD pathogenesis.

In this chapter, we aimed to identify key regulators of LRRK2 protein degradation by conducting a CRISPRi screen targeting UPS-relevant genes. Given that LRRK2 protein undergoes proteasomal degradation after kinase inhibition, we also conducted the screen after treatment with the LRRK2 kinase inhibitor MLi-2 to find kinase inhibitor-specific regulators. From the two different conditions, there were some overlaps between the significant hits that were significantly enriched in the collected population. These genes may contribute to general LRRK2 biology or could be broad regulators of gene expression for many genes. For example, PSMD4 showed up as a significant top hit for all of the screens conducted. This fits with the fact that PSMD4 is a component of the proteasome itself. The overlap also suggests that LRRK2 degradation under pharmacological intervention may utilize at least some of the pathways driving LRRK2 degradation under normal conditions.

The screen also identified SUMOylation and neddylation as pathways potentially involved in regulating LRRK2 protein levels. SUMOylation-relevant genes ranked higher under the non-kinase inhibitor-treated condition, while neddylation relevant genes ranked higher in the kinase inhibitor-treated condition. Using individual sgRNAs, we confirmed that SAE1, an E1

activating enzyme within the SUMOylation pathway, and UBA3, an E1 activating enzyme within the neddylation pathway regulate LRRK2 levels. UBA3 negatively regulates LRRK2 levels in the presence of MLi-2 while SAE1 does not, supporting the hypothesis that neddylation is involved in the kinase inhibitor relevant pathway while SUMOylation is not.

We found that the E3 ligase RBX1 within the neddylation pathway also negatively regulates LRRK2 levels. This result is in line with the hypothesis that neddylation could drive LRRK2 protein turnover. Surprisingly, the top hit PIAS2 within the SUMOylation pathway regulated LRRK level positively. This result failed to replicate the screen result. One potential explanation could be that PIAS2 might not be the essential E3 ligase that interacts with LRRK2, since multiple E3 ligases have been identified in the SUMOylation pathway while only two E1 enzymes and one E2 enzyme has been identified (52). Moreover, SUMOylation is also a process that frequently occurs in the nucleus, which is an uncommon place for LRRK2 protein (62). Therefore, LRRK2 might not be the protein directly SUMOylated. Downregulation of LRRK2 by PIAS2 knockdown could be due to a complex secondary effect of PIAS2 on SUMOylation.

This preliminary screen offers a starting point to understanding LRRK2 turnover. One immediate next step is to validate the screen hits with individual knockdowns in a cellular system expressing endogenous levels of LRRK2, something which we are now beginning to do using HALO-tagged genomic LRRK2. To investigate the mechanistic link between the two pathways, we would also want to know the factor that links these posttranslational modifications with LRRK2 protein level. To determine this, we can screen through a series of previously reported SUMOylation or neddylation substrates via sgRNA knockdown to see how they affect LRRK2 levels. For instance, neddylation is known to activate a group of cullin E3 ubiquitin ligases of which RBX1 can be a component, though RBX1 does not typically serve as the direct

substrate adaptor. We are also interested in how the SUMOylation and neddylation regulate LRRK2 kinase activity. With more understanding of the two pathways, we may be able to separate LRRK2 turnover from LRRK2 kinase inhibition and investigate whether LRRK2 toxicity is tied to its kinase activity or protein level.

Beyond following up on these two pathways, the screen also identified other potential LRRK2 protein regulators involved in alternate proteostasis pathways. Therefore, another future aim is to generate individual sgRNAs to validate other hits within the screen. For example, MAEA is another E3 ligase that showed up as a significant hit but is unrelated to SUMOylation and neddylation. The VCP-NPLOC-UFD1 complex, which promotes the degradation of polyubiquitinated proteins, also appeared as a significant hit in both DMSO and MLi-2-treated conditions (63). It would also be interesting to evaluate the bottom hits of the screen, which could be positively regulating LRRK2 levels. Furthermore, to get a more biologically relevant list of target genes, we can generate a cellular system with stably transfected CRISPRi machinery alongside reporter tagged endogenous LRRK2 to repeat the screen under conditions were LRRK2 is expressed at endogenous levels. We might also be interested in using the CRISPRa machinery to see how the overexpression of proteins impact LRRK2 turnover and how the gene list compares to the list of bottom hits for this screen.

Figures

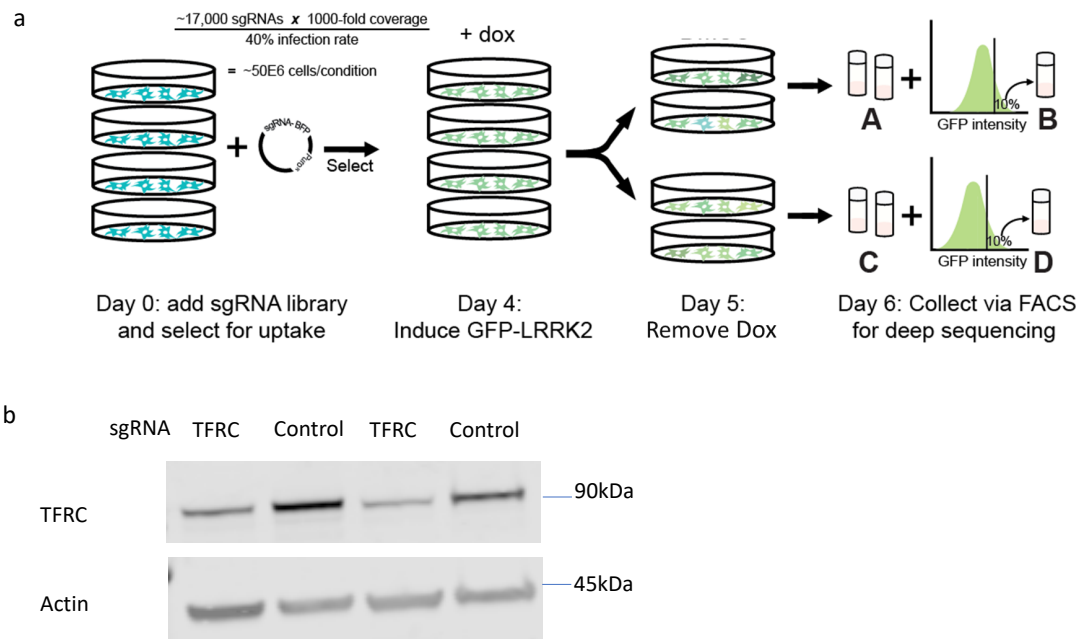

Figure 3.1: CRISPRi screening system overview a)Schematic of CRISPRi screen, ~3,500 genes were screened for their ability to regulate GFP-LRRK2 protein levels. sgRNA library (5 guides/gene, ~300 non-targeting guides) was introduced by viral transduction. Cells with the highest or lowest GFP intensity were FACS sorted and deep sequencing of these populations was performed and analyzed. b) Immunoblot for TFRC Knockdown in dox- GFP-LRRK2 cells. Dox- GFP-LRRK2 cells were lentivirally infected with an sgRNA targeting TFRC or an empty vector control. GFP-LRRK2 expression was induced by addition of doxycycline on Day 4 after infection. Cells were harvested 48 hrs after dox induction. Representative experiments shown, n=3 for TFRC KD.

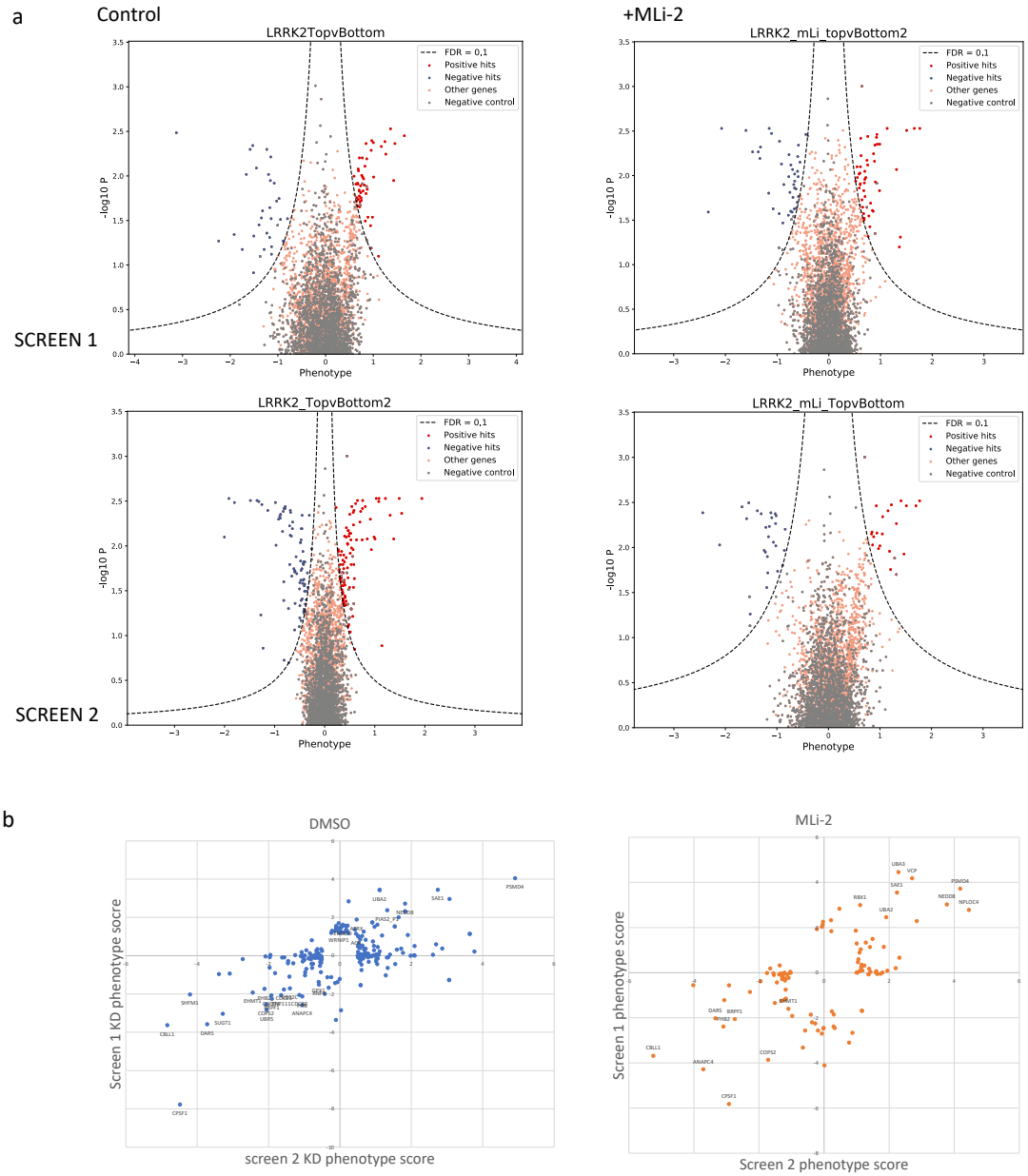

Figure 3.2: CRISPRi screen identified LRRK2 protein interactors. a) Volcano plots summarizing knockdown phenotypes and statistical significance (Mann-Whitney U test) for genes targeted in the screen. Positive hits increase in enrichment for top 30% GFP expressing cells. Negative hits increase in enrichment for bottom 30% GFP expressing cells. Dashed lines: cutoff for hit genes (FDR = 0.05). b) Scatter plot summarizing knockdown phenotypes (product score) across two screens for genes listed as hits in c) in either screen. Hits that show up in both screens are labeled with the gene's name.

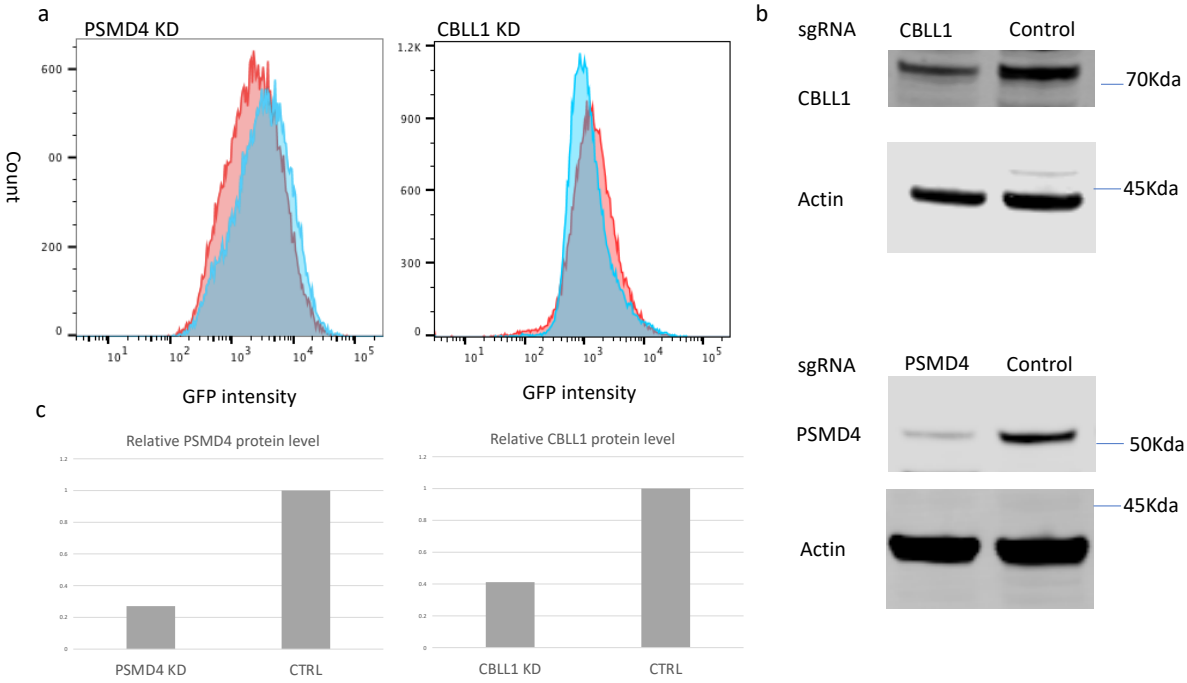

Figure 3.3: Individual sgRNA knockdown confirmed the effect of the CRISPRi screen on LRRK2 level change. a) Knockdown of the single top hit (PSMD4) vs bottom hit (CBLL1) in dox- GFP-LRRK2 cells. Dox- GFP-LRRK2 cells were lentivirally infected with an sgRNA targeting PSMD4, CBLL1 or an empty vector control. GFP-LRRK2 expression was induced by addition of doxycycline on Day 4 after infection. Cells were harvested 48 hrs after dox induction for FACs analysis. Representative experiments shown, n=3 for PSMD3 KD, n=2 for CBLL1 KD. b) Immunoblotting of a) showing PSMD4 and CBLL1 level change c) Quantification of b)

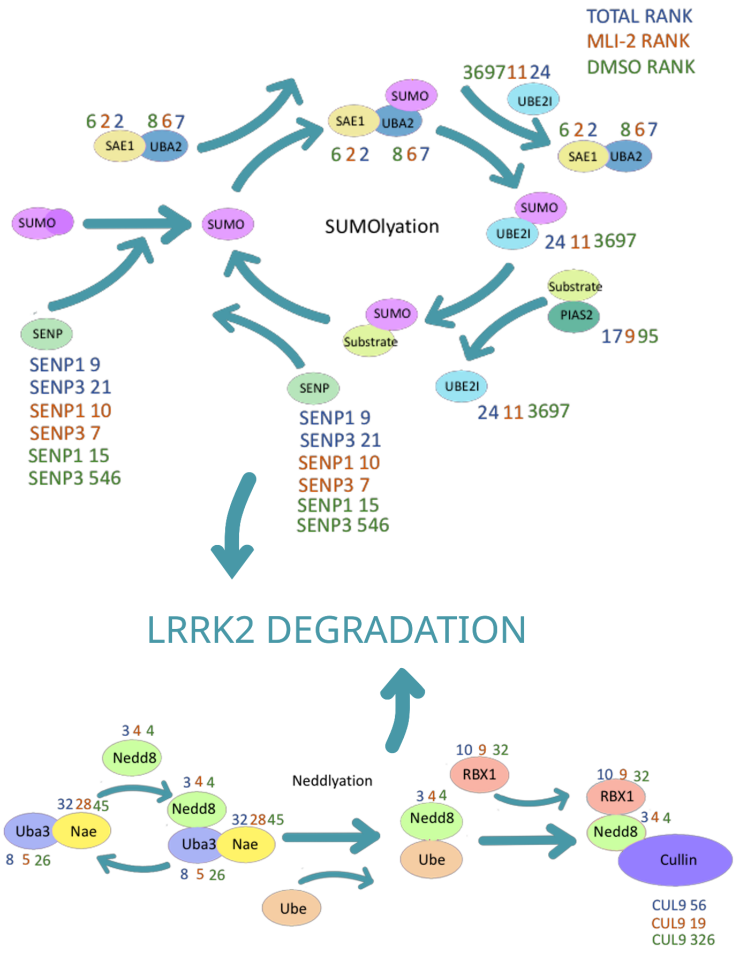

Figure 3.4: SUMOylation and neddylation are key regulatory pathway for LRRK2 turnover: Schematic of SUMOylation and neddylation pathway with ranks of hit genes in two condition combined, DMSO control condition and mLI-2 treated condition.

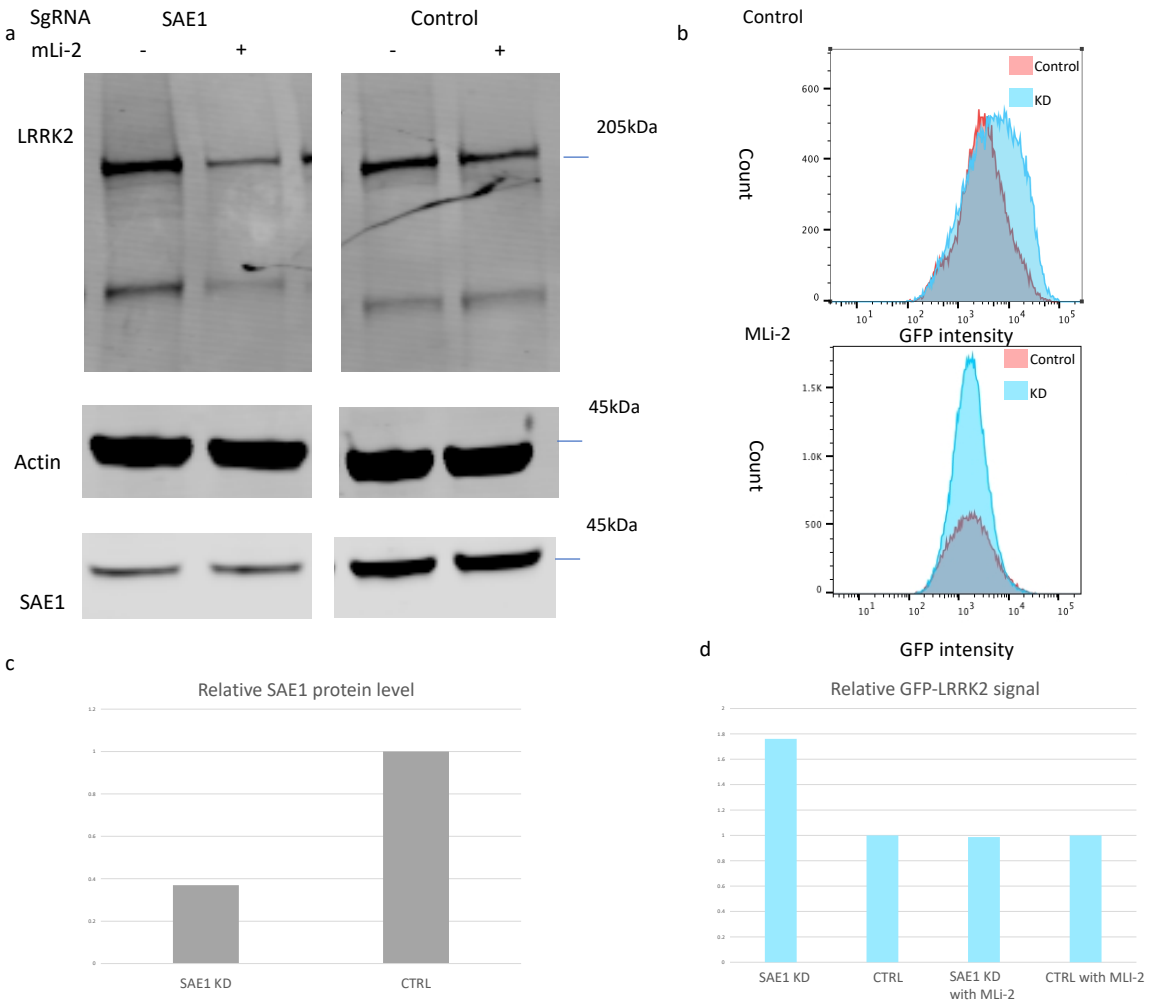

Figure: 3.5 Changes in LRRK2 expression with SAE1 Knockdown a) Immunoblot showing LRRK2 levels change relative to actin with SUMOylation (SAE1) relevant gene knockdowns). Dox- GFP-LRRK2 cells were lentivirally infected with an sgRNA targeting SAE1 or an empty vector control. GFP-LRRK2 expression was induced by addition of doxycycline on Day 2-4 after infection. mLI-2 was added to cells 24 hours after dox induction Cells were harvested 24 hours after mLi-2 treatment for analysis. Figure cropped for better visualization. Representative experiment shown, n=3 for SAE1 KD. b) Facs analysis showing histogram of GFP-LRRK fluorescent signal in a). c)Quantification of SAE1 efficiency in a) . d) Quantification of median GFP-LRRK2 level change in c)

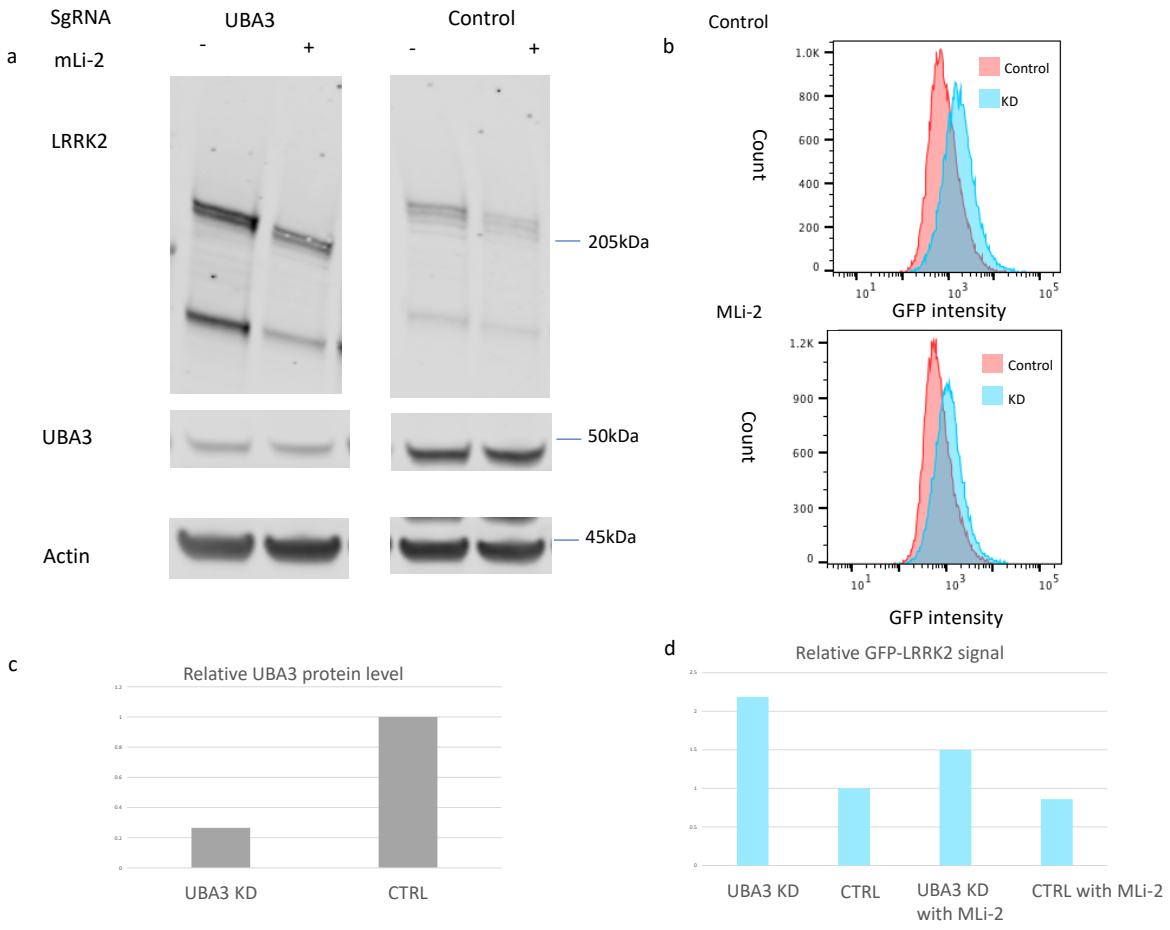

Figure 3.6 Changes in LRRK2 expression with UBA3 Knockdown a) Immunoblot showing LRRK2 levels change relative to actin with neddylation (UBA3) relevant gene knockdowns). Dox- GFP-LRRK2 cells were lentivirally infected with an sgRNA targeting UBA3 or an empty vector control. GFP-LRRK2 expression was induced by addition of doxycycline on Day 2-4 after infection. mLI-2 was added to cells 24 hours after dox induction Cells were harvested 24 hours after mLi-2 treatment for analysis. Figure cropped for better visualization. Representative experiments shown, n=2 b) Facs analysis showing histogram of GFP-LRRK fluorescent signal in a). c) Quantification UBA3 KD efficiency in a). d) Quantification of median GFP-LRRK2 level change in c)

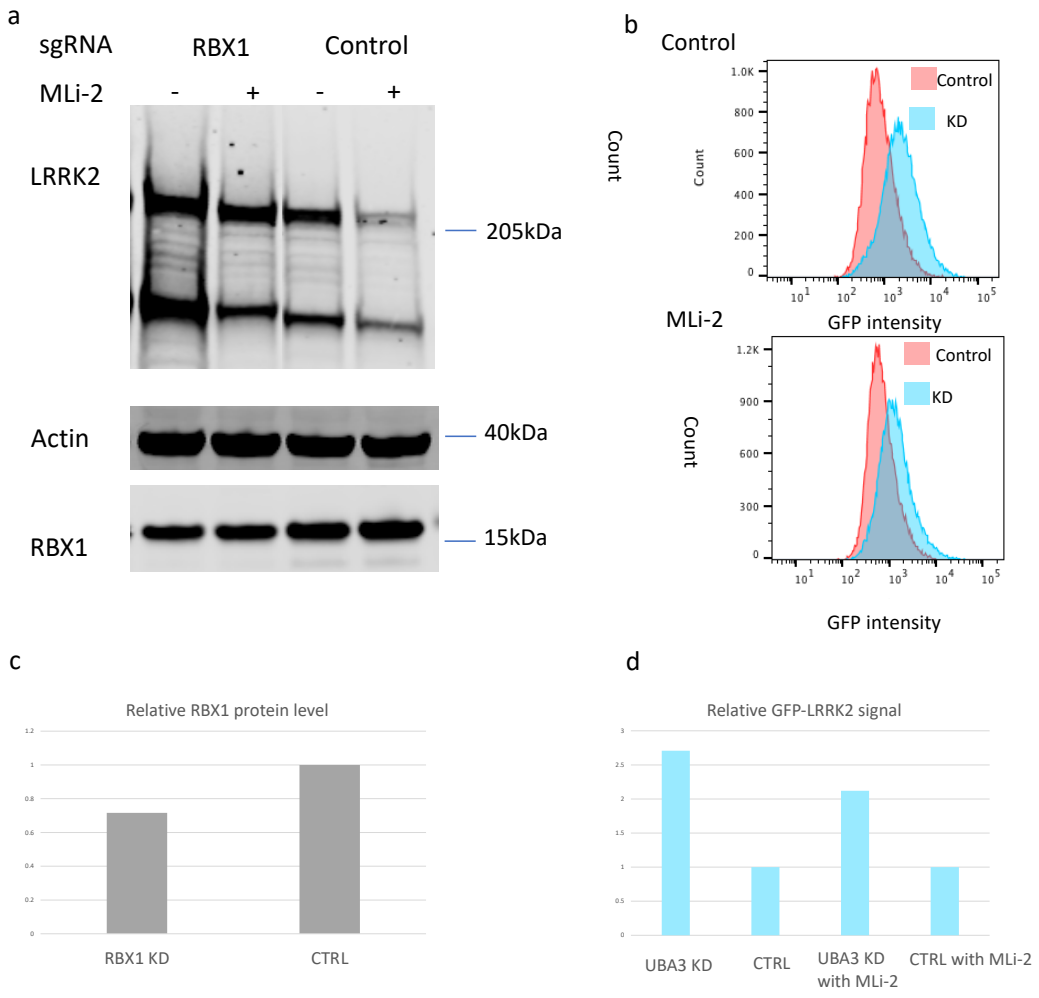

Figure 3.7 Changes in LRRK2 expression with RBXI Knockdown a) Immunoblot showing LRRK2 levels change relative to actin with RBX1 knockdowns and kinase inhibitor treatment. Dox- GFP-LRRK2 cells were lentivirally infected with an sgRNA targeting RBX1 or an empty vector control. GFP-LRRK2 expression was induced by addition of doxycycline on Day 2-4 after infection. mLI-2 was added to cells 24 hours after dox induction. Cells were harvested 24 hours after mLi-2 treatment for analysis. figure cropped for better visualization. Representative experiments shown, n=2 for RBX1 KD b) Flow cytometric histograms showing LRRK2 level changes with RBX1 knockdowns and kinase inhibitor treatment (mLi-2 treatment for 24 hours) in a). c)Quantification of RBX1 KD efficiency in a). d)Quantification of GFP-LRRK2 median level change in b)

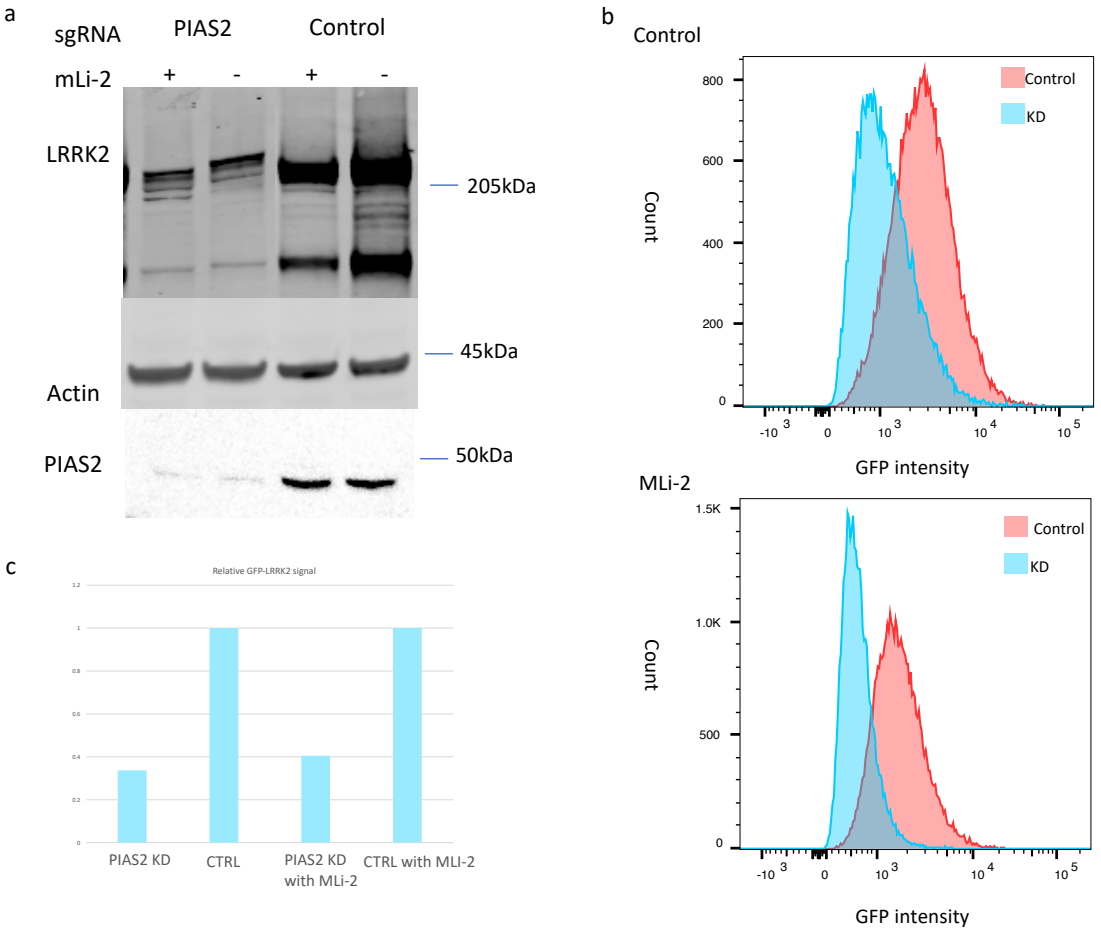

Figure 3.8 Changes in LRRK2 expression with PIAS2 Knockdown a) Immunoblot showing LRRK2 level changes relative to actin with PIAS2 knockdown and kinase inhibitor treatment. Dox- GFP-LRRK2 cells were lentivirally infected with an sgRNA targeting PIAS2 or an empty vector control. GFP-LRRK2 expression was induced by addition of doxycycline on Day 2-4 after infection. mLI-2 was added to cells 24 hours after dox induction Cells were harvested 24 hours after mLi-2 treatment for analysis. PIAS2 visualized with chemiluminescent secondary antibody, other proteins visualized with fluorescent secondary antibody. Representative experiments shown, n=4 for PIAS2 KD b) Flow cytometric histograms showing LRRK2 level changes with PIAS2 Knockdown and kinase inhibitor treatment (mLi-2 treatment for 24 hours) in a). c) Quantification of LRRK2 levels change in b).

Acknowledgment

Chapter 3 of this thesis contains unpublished data co-authored with Biswarathan Ramani at the Martin Kampmann lab from UCSF. The thesis author was the primary researcher of this chapter.

REFERENCES

1) Tysnes, OB., Storstein, A. Epidemiology of Parkinson's disease. *J Neural Transm* **124,** 901–905 (2017). https://doi.org/10.1007/s00702-017-1686-y

2) Sezgin, M., Bilgic, B., Tinaz, S., & Emre, M. (2019). Parkinson's Disease Dementia and Lewy Body Disease. *Seminars in neurology*, *39*(2), 274–282. https://doi.org/10.1055/s-0039-1678579

3) Wakabayashi, K., Tanji, K., Odagiri, S., Miki, Y., Mori, F., & Takahashi, H. (2013). The Lewy body in Parkinson's disease and related neurodegenerative disorders. *Molecular neurobiology*, *47*(2), 495–508. https://doi.org/10.1007/s12035-012-8280-y

4) Lashuel, H. A., Petre, B. M., Wall, J., Simon, M., Nowak, R. J., Walz, T., & Lansbury, P. T., Jr (2002). Alpha-synuclein, especially the Parkinson's disease-associated mutants, forms pore-like annular and tubular protofibrils. *Journal of molecular biology*, *322*(5), 1089–1102. https://doi.org/10.1016/s0022-2836(02)00735-0

5) Olanow, C. W., Perl, D. P., DeMartino, G. N., & McNaught, K. S. (2004). Lewy-body formation is an aggresome-related process: a hypothesis. *The Lancet. Neurology*, *3*(8), 496–503. https://doi.org/10.1016/S1474-4422(04)00827-0

6) Corti, O., Lesage, S., & Brice, A. (2011). What genetics tells us about the causes and mechanisms of Parkinson's disease. *Physiological reviews*, *91*(4), 1161–1218. https://doi.org/10.1152/physrev.00022.2010

7) Rui, Q., Ni, H., Li, D., Gao, R., & Chen, G. (2018). The Role of LRRK2 in Neurodegeneration of Parkinson Disease. *Current neuropharmacology*, *16*(9), 1348–1357. https://doi.org/10.2174/1570159X16666180222165418

8) Gilks, W. P., Abou-Sleiman, P. M., Gandhi, S., Jain, S., Singleton, A., Lees, A. J., Shaw, K., Bhatia, K. P., Bonifati, V., Quinn, N. P., Lynch, J., Healy, D. G., Holton, J. L., Revesz, T., & Wood, N. W. (2005). A common LRRK2 mutation in idiopathic Parkinson's disease. *Lancet (London, England)*, *365*(9457), 415–416. https://doi.org/10.1016/S0140-6736(05)17830-1

9) Healy, D. G., Falchi, M., O'Sullivan, S. S., Bonifati, V., Durr, A., Bressman, S., Brice, A., Aasly, J., Zabetian, C. P., Goldwurm, S., Ferreira, J. J., Tolosa, E., Kay, D. M., Klein, C., Williams, D. R., Marras, C., Lang, A. E., Wszolek, Z. K., Berciano, J., Schapira, A. H., … International LRRK2 Consortium (2008). Phenotype, genotype, and worldwide genetic penetrance of LRRK2-associated Parkinson's disease: a case-control study. *The Lancet. Neurology*, *7*(7), 583–590. https://doi.org/10.1016/S1474-4422(08)70117-0

10) Marder, K., Wang, Y., Alcalay, R. N., Mejia-Santana, H., Tang, M. X., Lee, A., Raymond, D., Mirelman, A., Saunders-Pullman, R., Clark, L., Ozelius, L., Orr-Urtreger, A., Giladi, N., Bressman, S., & LRRK2 Ashkenazi Jewish Consortium (2015). Age-

specific penetrance of LRRK2 G2019S in the Michael J. Fox Ashkenazi Jewish LRRK2 Consortium. *Neurology*, *85*(1), 89–95. https://doi.org/10.1212/WNL.0000000000001708

11) Simón-Sánchez, J., Schulte, C., Bras, J. M., Sharma, M., Gibbs, J. R., Berg, D., Paisan-Ruiz, C., Lichtner, P., Scholz, S. W., Hernandez, D. G., Krüger, R., Federoff, M., Klein, C., Goate, A., Perlmutter, J., Bonin, M., Nalls, M. A., Illig, T., Gieger, C., Houlden, H., … Gasser, T. (2009). Genome-wide association study reveals genetic risk underlying Parkinson's disease. *Nature genetics*, *41*(12), 1308–1312. https://doi.org/10.1038/ng.487

12) West, A. B., Moore, D. J., Choi, C., Andrabi, S. A., Li, X., Dikeman, D., Biskup, S., Zhang, Z., Lim, K. L., Dawson, V. L., & Dawson, T. M. (2007). Parkinson's disease-associated mutations in LRRK2 link enhanced GTP-binding and kinase activities to neuronal toxicity. *Human molecular genetics*, *16*(2), 223–232. https://doi.org/10.1093/hmg/ddl471

13) Kluss, J. H., Mamais, A., & Cookson, M. R. (2019). LRRK2 links genetic and sporadic Parkinson's disease. *Biochemical Society transactions*, *47*(2), 651–661. https://doi.org/10.1042/BST20180462

14) Schmidt, S. H., Knape, M. J., Boassa, D., Mumdey, N., Kornev, A. P., Ellisman, M. H., Taylor, S. S., & Herberg, F. W. (2019). The dynamic switch mechanism that leads to activation of LRRK2 is embedded in the DFGψ motif in the kinase domain. *Proceedings of the National Academy of Sciences of the United States of America*, *116*(30), 14979–14988. https://doi.org/10.1073/pnas.1900289116

15) Ito, G., Okai, T., Fujino, G., Takeda, K., Ichijo, H., Katada, T., & Iwatsubo, T. (2007). GTP binding is essential to the protein kinase activity of LRRK2, a causative gene product for familial Parkinson's disease. *Biochemistry*, *46*(5), 1380–1388. https://doi.org/10.1021/bi061960m

16) Deniston, C. K., Salogiannis, J., Mathea, S., Snead, D. M., Lahiri, I., Matyszewski, M., Donosa, O., Watanabe, R., Böhning, J., Shiau, A. K., Knapp, S., Villa, E., Reck-Peterson, S. L., & Leschziner, A. E. (2020). Structure of LRRK2 in Parkinson's disease and model for microtubule interaction. *Nature*, *588*(7837), 344–349. https://doi.org/10.1038/s41586-020-2673-2

17) Usmani, A., Shavarebi, F., & Hiniker, A. (2021). The Cell Biology of LRRK2 in Parkinson's Disease. *Molecular and cellular biology*, *41*(5), e00660-20. https://doi.org/10.1128/MCB.00660-20

18) West, A. B., Moore, D. J., Biskup, S., Bugayenko, A., Smith, W. W., Ross, C. A., Dawson, V. L., & Dawson, T. M. (2005). Parkinson's disease-associated mutations in leucine-rich repeat kinase 2 augment kinase activity. *Proceedings of the National Academy of Sciences of the United States of America*, *102*(46), 16842–16847. https://doi.org/10.1073/pnas.0507360102

19) Greggio, E., Jain, S., Kingsbury, A., Bandopadhyay, R., Lewis, P., Kaganovich, A., van der Brug, M. P., Beilina, A., Blackinton, J., Thomas, K. J., Ahmad, R., Miller, D. W., Kesavapany, S., Singleton, A., Lees, A., Harvey, R. J., Harvey, K., & Cookson, M. R. (2006). Kinase activity is required for the toxic effects of mutant LRRK2/dardarin. *Neurobiology of disease*, *23*(2), 329–341. https://doi.org/10.1016/j.nbd.2006.04.001

20) Lee, B. D., Shin, J. H., VanKampen, J., Petrucelli, L., West, A. B., Ko, H. S., Lee, Y. I., Maguire-Zeiss, K. A., Bowers, W. J., Federoff, H. J., Dawson, V. L., & Dawson, T. M. (2010). Inhibitors of leucine-rich repeat kinase-2 protect against models of Parkinson's disease. *Nature medicine*, *16*(9), 998–1000. https://doi.org/10.1038/nm.2199

21) Di Maio, R., Hoffman, E. K., Rocha, E. M., Keeney, M. T., Sanders, L. H., De Miranda, B. R., Zharikov, A., Van Laar, A., Stepan, A. F., Lanz, T. A., Kofler, J. K., Burton, E. A., Alessi, D. R., Hastings, T. G., & Greenamyre, J. T. (2018). LRRK2 activation in idiopathic Parkinson's disease. *Science translational medicine*, *10*(451), eaar5429. https://doi.org/10.1126/scitranslmed.aar5429

22) Herzig, M. C., Kolly, C., Persohn, E., Theil, D., Schweizer, T., Hafner, T., Stemmelen, C., Troxler, T. J., Schmid, P., Danner, S., Schnell, C. R., Mueller, M., Kinzel, B., Grevot, A., Bolognani, F., Stirn, M., Kuhn, R. R., Kaupmann, K., van der Putten, P. H., Rovelli, G., … Shimshek, D. R. (2011). LRRK2 protein levels are determined by kinase function and are crucial for kidney and lung homeostasis in mice. *Human molecular genetics*, *20*(21), 4209–4223. https://doi.org/10.1093/hmg/ddr348

23) Tong, Y., Yamaguchi, H., Giaime, E., Boyle, S., Kopan, R., Kelleher, R. J., 3rd, & Shen, J. (2010). Loss of leucine-rich repeat kinase 2 causes impairment of protein degradation pathways, accumulation of alpha-synuclein, and apoptotic cell death in aged mice. *Proceedings of the National Academy of Sciences of the United States of America*, *107*(21), 9879–9884. https://doi.org/10.1073/pnas.1004676107

24) Giaime, E., Tong, Y., Wagner, L. K., Yuan, Y., Huang, G., & Shen, J. (2017). Age-Dependent Dopaminergic Neurodegeneration and Impairment of the Autophagy-Lysosomal Pathway in LRRK-Deficient Mice. *Neuron*, *96*(4), 796–807.e6. https://doi.org/10.1016/j.neuron.2017.09.036

25) Volta, M., & Melrose, H. (2017). LRRK2 mouse models: dissecting the behavior, striatal neurochemistry and neurophysiology of PD pathogenesis. *Biochemical Society transactions*, *45*(1), 113–122. https://doi.org/10.1042/BST20160238

26) Berger, Z., Smith, K. A., & Lavoie, M. J. (2010). Membrane localization of LRRK2 is associated with increased formation of the highly active LRRK2 dimer and changes in its phosphorylation. *Biochemistry*, *49*(26), 5511–5523. https://doi.org/10.1021/bi100157u

27) Marchand, A., Drouyer, M., Sarchione, A., Chartier-Harlin, M. C., & Taymans, J. M. (2020). LRRK2 Phosphorylation, More Than an Epiphenomenon. *Frontiers in neuroscience*, *14*, 527. https://doi.org/10.3389/fnins.2020.00527

28) Sheng, Z., Zhang, S., Bustos, D., Kleinheinz, T., Le Pichon, C. E., Dominguez, S. L., Solanoy, H. O., Drummond, J., Zhang, X., Ding, X., Cai, F., Song, Q., Li, X., Yue, Z., van der Brug, M. P., Burdick, D. J., Gunzner-Toste, J., Chen, H., Liu, X., Estrada, A. A., … Zhu, H. (2012). Ser1292 autophosphorylation is an indicator of LRRK2 kinase activity and contributes to the cellular effects of PD mutations. *Science translational medicine*, *4*(164), 164ra161. https://doi.org/10.1126/scitranslmed.3004485

29) Steger, M., Tonelli, F., Ito, G., Davies, P., Trost, M., Vetter, M., Wachter, S., Lorentzen, E., Duddy, G., Wilson, S., Baptista, M. A., Fiske, B. K., Fell, M. J., Morrow, J. A., Reith, A. D., Alessi, D. R., & Mann, M. (2016). Phosphoproteomics reveals that Parkinson's disease kinase LRRK2 regulates a subset of Rab GTPases. *eLife*, *5*, e12813. https://doi.org/10.7554/eLife.12813

30) Steger, M., Diez, F., Dhekne, H. S., Lis, P., Nirujogi, R. S., Karayel, O., Tonelli, F., Martinez, T. N., Lorentzen, E., Pfeffer, S. R., Alessi, D. R., & Mann, M. (2017). Systematic proteomic analysis of LRRK2-mediated Rab GTPase phosphorylation establishes a connection to ciliogenesis. *eLife*, *6*, e31012. https://doi.org/10.7554/eLife.31012

31) Purlyte, E., Dhekne, H. S., Sarhan, A. R., Gomez, R., Lis, P., Wightman, M., Martinez, T. N., Tonelli, F., Pfeffer, S. R., & Alessi, D. R. (2019). Rab29 activation of the Parkinson's disease-associated LRRK2 kinase. *The EMBO journal*, *38*(2), e101237. https://doi.org/10.15252/embj.2018101237

32) Fell, M. J., Mirescu, C., Basu, K., Cheewatrakoolpong, B., DeMong, D. E., Ellis, J. M., Hyde, L. A., Lin, Y., Markgraf, C. G., Mei, H., Miller, M., Poulet, F. M., Scott, J. D., Smith, M. D., Yin, Z., Zhou, X., Parker, E. M., Kennedy, M. E., & Morrow, J. A. (2015). MLi-2, a Potent, Selective, and Centrally Active Compound for Exploring the Therapeutic Potential and Safety of LRRK2 Kinase Inhibition. *The Journal of pharmacology and experimental therapeutics*, *355*(3), 397–409. https://doi.org/10.1124/jpet.115.227587

33) Fuji, R. N., Flagella, M., Baca, M., Baptista, M. A., Brodbeck, J., Chan, B. K., Fiske, B. K., Honigberg, L., Jubb, A. M., Katavolos, P., Lee, D. W., Lewin-Koh, S. C., Lin, T., Liu, X., Liu, S., Lyssikatos, J. P., O'Mahony, J., Reichelt, M., Roose-Girma, M., Sheng, Z., … Watts, R. J. (2015). Effect of selective LRRK2 kinase inhibition on nonhuman primate lung. *Science translational medicine*, *7*(273), 273ra15. https://doi.org/10.1126/scitranslmed.aaa3634

34) Weygant, N., Qu, D., Berry, W. L., May, R., Chandrakesan, P., Owen, D. B., Sureban, S. M., Ali, N., Janknecht, R., & Houchen, C. W. (2014). Small molecule kinase inhibitor LRRK2-IN-1 demonstrates potent activity against colorectal and pancreatic cancer through inhibition of doublecortin-like kinase 1. *Molecular cancer*, *13*, 103. https://doi.org/10.1186/1476-4598-13-103

35) Wu, P., Nielsen, T. E., & Clausen, M. H. (2015). FDA-approved small-molecule kinase inhibitors. *Trends in pharmacological sciences*, *36*(7), 422–439. https://doi.org/10.1016/j.tips.2015.04.005

36) Baptista, M., Merchant, K., Barrett, T., Bhargava, S., Bryce, D. K., Ellis, J. M., Estrada, A. A., Fell, M. J., Fiske, B. K., Fuji, R. N., Galatsis, P., Henry, A. G., Hill, S., Hirst, W., Houle, C., Kennedy, M. E., Liu, X., Maddess, M. L., Markgraf, C., Mei, H., … Sherer, T. B. (2020). LRRK2 inhibitors induce reversible changes in nonhuman primate lungs without measurable pulmonary deficits. *Science translational medicine*, *12*(540), eaav0820. https://doi.org/10.1126/scitranslmed.aav0820

37) Lobbestael, E., Civiero, L., De Wit, T., Taymans, J. M., Greggio, E., & Baekelandt, V. (2016). Pharmacological LRRK2 kinase inhibition induces LRRK2 protein destabilization and proteasomal degradation. *Scientific reports*, *6*, 33897. https://doi.org/10.1038/srep33897

38) Dzamko, N., Deak, M., Hentati, F., Reith, A. D., Prescott, A. R., Alessi, D. R., & Nichols, R. J. (2010). Inhibition of LRRK2 kinase activity leads to dephosphorylation of Ser(910)/Ser(935), disruption of 14-3-3 binding and altered cytoplasmic localization. *The Biochemical journal*, *430*(3), 405–413. https://doi.org/10.1042/BJ20100784

39) Jing Zhao, Tyler P. Molitor, J. William Langston, R. Jeremy Nichols; LRRK2 dephosphorylation increases its ubiquitination. *Biochem J* 1 July 2015; 469 (1): 107–120. doi: https://doi.org/10.1042/BJ20141305

40) Cook, D. A., Kannarkat, G. T., Cintron, A. F., Butkovich, L. M., Fraser, K. B., Chang, J., Grigoryan, N., Factor, S. A., West, A. B., Boss, J. M., & Tansey, M. G. (2017). LRRK2 levels in immune cells are increased in Parkinson's disease. *NPJ Parkinson's disease*, *3*, 11. https://doi.org/10.1038/s41531-017-0010-8

41) Skibinski, G., Nakamura, K., Cookson, M. R., & Finkbeiner, S. (2014). Mutant LRRK2 toxicity in neurons depends on LRRK2 levels and synuclein but not kinase activity or inclusion bodies. *The Journal of neuroscience : the official journal of the Society for Neuroscience*, *34*(2), 418–433. https://doi.org/10.1523/JNEUROSCI.2712-13.2014

42) Orenstein, S. J., Kuo, S. H., Tasset, I., Arias, E., Koga, H., Fernandez-Carasa, I., Cortes, E., Honig, L. S., Dauer, W., Consiglio, A., Raya, A., Sulzer, D., & Cuervo, A. M. (2013). Interplay of LRRK2 with chaperone-mediated autophagy. *Nature neuroscience*, *16*(4), 394–406. https://doi.org/10.1038/nn.3350

43) Finkbeiner S. (2020). The Autophagy Lysosomal Pathway and Neurodegeneration. *Cold Spring Harbor perspectives in biology*, *12*(3), a033993. https://doi.org/10.1101/cshperspect.a033993

44) Nandi, D., Tahiliani, P., Kumar, A., & Chandu, D. (2006). The ubiquitin-proteasome system. *Journal of biosciences*, *31*(1), 137–155. https://doi.org/10.1007/BF02705243

45) Ko, H. S., Bailey, R., Smith, W. W., Liu, Z., Shin, J. H., Lee, Y. I., Zhang, Y. J., Jiang, H., Ross, C. A., Moore, D. J., Patterson, C., Petrucelli, L., Dawson, T. M., & Dawson, V. L. (2009). CHIP regulates leucine-rich repeat kinase-2 ubiquitination, degradation, and toxicity. *Proceedings of the National Academy of Sciences of the United States of America*, *106*(8), 2897–2902. https://doi.org/10.1073/pnas.0810123106

46) Nucifora, F. C., Jr, Nucifora, L. G., Ng, C. H., Arbez, N., Guo, Y., Roby, E., Shani, V., Engelender, S., Wei, D., Wang, X. F., Li, T., Moore, D. J., Pletnikova, O., Troncoso, J. C., Sawa, A., Dawson, T. M., Smith, W., Lim, K. L., & Ross, C. A. (2016). Ubiqutination via K27 and K29 chains signals aggregation and neuronal protection of LRRK2 by WSB1. *Nature communications*, *7*, 11792. https://doi.org/10.1038/ncomms11792

47) Stormo, A., Shavarebi, F., FitzGibbon, M., Earley, E. M., Ahrendt, H., Lum, L. S., Verschueren, E., Swaney, D. L., Skibinski, G., Ravisankar, A., van Haren, J., Davis, E. J., Johnson, J. R., Von Dollen, J., Balen, C., Porath, J., Crosio, C., Mirescu, C., Iaccarino, C., Dauer, W. T., … Hiniker, A. (2022). The E3 ligase TRIM1 ubiquitinates LRRK2 and controls its localization, degradation, and toxicity. *The Journal of cell biology*, *221*(4), e202010065. https://doi.org/10.1083/jcb.202010065

48) Toyofuku, T., Okamoto, Y., Ishikawa, T., Sasawatari, S., & Kumanogoh, A. (2020). LRRK2 regulates endoplasmic reticulum-mitochondrial tethering through the PERK-mediated ubiquitination pathway. *The EMBO journal*, *39*(2), e100875. https://doi.org/10.15252/embj.2018100875

49) Ding, X., Barodia, S. K., Ma, L., & Goldberg, M. S. (2017). Fbxl18 targets LRRK2 for proteasomal degradation and attenuates cell toxicity. *Neurobiology of disease*, *98*, 122–136. https://doi.org/10.1016/j.nbd.2016.11.004

50) Edkins A. L. (2015). CHIP: a co-chaperone for degradation by the proteasome. *Sub-cellular biochemistry*, *78*, 219–242. https://doi.org/10.1007/978-3-319-11731-7_11

51) Zhao, J., Molitor, T. P., Langston, J. W., & Nichols, R. J. (2015). LRRK2 dephosphorylation increases its ubiquitination. *The Biochemical journal*, *469*(1), 107–120. https://doi.org/10.1042/BJ20141305

52) Müller, S., Hoege, C., Pyrowolakis, G., & Jentsch, S. (2001). SUMO, ubiquitin's mysterious cousin. *Nature reviews. Molecular cell biology*, *2*(3), 202–210. https://doi.org/10.1038/35056591

53) van der Veen, A. G., & Ploegh, H. L. (2012). Ubiquitin-like proteins. *Annual review of biochemistry*, *81*, 323–357. https://doi.org/10.1146/annurev-biochem-093010-153308

54) Shi, X., Du, Y., Li, S., & Wu, H. (2022). The Role of SUMO E3 Ligases in Signaling Pathway of Cancer Cells. *International journal of molecular sciences*, *23*(7), 3639. https://doi.org/10.3390/ijms23073639

55) Rabut, G., & Peter, M. (2008). Function and regulation of protein neddylation. 'Protein modifications: beyond the usual suspects' review series. *EMBO reports*, *9*(10), 969–976. https://doi.org/10.1038/embor.2008.183

56) Choo, Y. S., Vogler, G., Wang, D., Kalvakuri, S., Iliuk, A., Tao, W. A., Bodmer, R., & Zhang, Z. (2012). Regulation of parkin and PINK1 by neddylation. *Human molecular genetics*, *21*(11), 2514–2523. https://doi.org/10.1093/hmg/dds070

57) Choo, Y. S., Vogler, G., Wang, D., Kalvakuri, S., Iliuk, A., Tao, W. A., Bodmer, R., & Zhang, Z. (2012). Regulation of parkin and PINK1 by neddylation. *Human molecular genetics*, *21*(11), 2514–2523. https://doi.org/10.1093/hmg/dds070

58) Verma, D. K., Ghosh, A., Ruggiero, L., Cartier, E., Janezic, E., Williams, D., Jung, E. G., Moore, M., Seo, J. B., & Kim, Y. H. (2020). The SUMO Conjugase Ubc9 Protects Dopaminergic Cells from Cytotoxicity and Enhances the Stability of α-Synuclein in Parkinson's Disease Models. eNeuro, 7(5), ENEURO.0134-20.2020. https://doi.org/10.1523/ENEURO.0134-20.2020

59) Gilbert, L. A., Larson, M. H., Morsut, L., Liu, Z., Brar, G. A., Torres, S. E., Stern-Ginossar, N., Brandman, O., Whitehead, E. H., Doudna, J. A., Lim, W. A., Weissman, J. S., & Qi, L. S. (2013). CRISPR-mediated modular RNA-guided regulation of transcription in eukaryotes. *Cell*, *154*(2), 442–451. https://doi.org/10.1016/j.cell.2013.06.044

60) Tian, R., Gachechiladze, M. A., Ludwig, C. H., Laurie, M. T., Hong, J. Y., Nathaniel, D., Prabhu, A. V., Fernandopulle, M. S., Patel, R., Abshari, M., Ward, M. E., & Kampmann, M. (2019). CRISPR Interference-Based Platform for Multimodal Genetic Screens in Human iPSC-Derived Neurons. *Neuron*, *104*(2), 239–255.e12. https://doi.org/10.1016/j.neuron.2019.07.014

61) Horlbeck, M. A., Gilbert, L. A., Villalta, J. E., Adamson, B., Pak, R. A., Chen, Y., Fields, A. P., Park, C. Y., Corn, J. E., Kampmann, M., & Weissman, J. S. (2016). Compact and highly active next-generation libraries for CRISPR-mediated gene repression and activation. *eLife*, *5*, e19760. https://doi.org/10.7554/eLife.19760

62) Saitoh, N., Uchimura, Y., Tachibana, T., Sugahara, S., Saitoh, H., & Nakao, M. (2006). In situ SUMOylation analysis reveals a modulatory role of RanBP2 in the nuclear rim and PML bodies. *Experimental cell research*, *312*(8), 1418–1430. https://doi.org/10.1016/j.yexcr.2006.01.013

63) Wolf, D. H., & Stolz, A. (2012). The Cdc48 machine in endoplasmic reticulum associated protein degradation. *Biochimica et biophysica acta*, *1823*(1), 117–124. https://doi.org/10.1016/j.bbamcr.2011.09.002